This is to certify that the

thesis entitled

AN EXPERIMENTAL STUDY OF FATIGUE
CRACK GROWTH FROM FASTENER HOLES
REPAIRED BY COLDWORKING

presented by

WALTER JOSEPH CESARZ

has been accepted towards fulfillment
of the requirements for

M.S. degree in Mechanics

William N Sharpe

Major professor

Date July 21, 1978

O-7639

AN EXPERIMENTAL STUDY OF FATIGUE
CRACK GROWTH FROM FASTENER HOLES
REPAIRED BY COLDWORKING

By

Walter J. Cesarz, Jr.

A THESIS

Submitted to
Michigan State University
in partial fulfillment of the requirements
for the degree of

MASTER OF SCIENCE

Department of Metallurgy, Mechanics,
and Material Science

1978

2 113456

ABSTRACT

AN EXPERIMENTAL STUDY OF FATIGUE CRACK GROWTH FROM FASTENER HOLES REPAIRED BY COLDWORKING

By

Walter J. Cesarz, Jr.

This report describes the experimental studies investigating the crack behavior for a hole which had a 1mm fatigue crack started before the hole was coldworked. The data was compared to the results of Chandawanich (1) for a hole which was not damaged before coldworking.

Fatigue tests were restricted to 0.125 inch (3.2mm) thick specimens made from type 7075-T6 aluminum sheet. A hole size of 0.195 inches (4.98mm) was used and the specimens were tested with a constant-amplitude cyclic load which varied from 7500 lbs (33375N) to 750 lbs (3337.5N) with a frequency of 15 Hz.

Results showed that the hole which was not damaged before coldworking required 3½ times more cycles to grow a crack to 6mm than the hole which was damaged before coldworking. The sleeve left in the damaged hole after coldworking seemed to make no difference in crack growth. Results also showed that the residual strains were slightly smaller around the damaged hole as compared to the undamaged hole.

ACKNOWLEDGMENTS

I would like to thank my major professor Dr. William N. Sharpe, Jr. for his suggestions and guidance in both areas of experimentation and writing of this thesis.

Dr. G. L. Cloud was also very helpful during this investigation along with Mr. D. R. Martin and Mr. D. L. Koch, and I wish to extend my appreciation to them also.

A special thanks goes to my family and to Miss C. D. Langenberg for their patience and encouragement during my study.

TABLE OF CONTENTS

TABLE OF CONTENTS--continued

CHAPTER Page

LIST OF TABLES

LIST OF FIGURES

LIST OF FIGURES--continued

CHAPTER 1

INTRODUCTION

Flaw-induced fracture has been responsible for failures in a wide variety of engineering structures such as tanks, pressure vessels, ships and turbine blades. For many years both commercial and military aircraft have been plagued with the problem of very small fatigue cracks originating from bolt or rivet holes. The flight hours on these aircraft are then reduced due to the damage caused by the fatigue cracks. One means of improving the fatigue life of these structures is to inhibit the growth of flaws emanating from the fastener holes by prestressing the metal around the hole by coldworking with an oversized mandrel. This affects the material in two ways. First it introduces a tangle of dislocations which restricts further dislocation glide, and second it causes residual elastic compressive strains to form near the cold-worked areas. Both of the above increase the stress required to produce the local yielding that leads to crack initiation. Chandawanich (1) has shown in a recent study that mandrelizing a hole helps to slow crack growth. Other investigators such as E. R. Speakman (2) and Gerber-Fuchs (3) have also shown the advantages coldworking has on improving fatigue life.

1.1 Purpose

The purpose of this research was to study the effect mandrelizing has on the growth of an existing crack; i.e., a fatigue crack was first formed alongside a hole followed by coldworking. The growth of the existing crack was then studied. The results of this investigation may be used to determine how well a cracked hole can be repaired through coldworking. This investigation includes the study of residual strain fields, crack propagation behavior, and the stress intensity factor.

Residual strain beside the coldworked holes was measured by the Moiré technique and the stress intensity factor was determined from a laser interferometry method known as the interferometric displacement gage. The Moiré effect, produced by mechanical interference, has been known for a very long time and a straight-forward analysis can be used to relate the interference pattern to displacement and/or strain. In contrast the interferometric displacement gage is a comparatively recent invention and when interfaced with computer techniques the system becomes a sophisticated tool.

Experimental results of this investigation were compared to the results of Chandawanich (1) since the specimen dimensions and testing procedures were similar. In the investigation of Chandawanich the holes were mandrelized before fatigue cracks were grown, in contrast to growing the cracks before coldworking as in this report. The comparisons are presented in graphical form where the differences and similarities can easily be seen between the two procedures.

1.2 Organization of Thesis

The material specifications and preparation are given in Chapter 2 along with a description of the coldworking process. In Chapter 3 the Moiré technique is described. This includes an explanation of data reduction using Moiré analysis and laboratory techniques such as grid application. Also in Chapter 3 is a discussion on the experimental procedures for fatigue testing and the interferometric displacement gage.

Chapter 4 contains the crack growth data and discussion. Included is information on the specimens for which the sleeves were left in place after coldworking.

Strain measurement is the topic of Chapter 5 which is a discussion of residual strains around a coldworked hole. The strains were found by use of the Moiré technique described in Chapter 3.

Chapter 6 includes crack shape curves and information on the crack mouth displacements.

The stress intensity factor versus crack length is presented in Chapter 7 for the mandrelized hole. These results were obtained with the interferometric displacement gage.

The findings of this research are considered in Chapter 8 which concludes the thesis.

CHAPTER 2

MATERIAL DESCRIPTION

2.1 <u>Material Specification and Preparation</u>

2.1.1 Material Specifications

Aluminum type 7075-T6 was the material tested. The sheet form was used, and the thickness was 1/8 inch (3.20mm). This type of aluminum is characterized as having high strength, excellent abrasion resistance, and it ranks fair for corrosion resistance. The above characteristics of this aluminum make it a favorable material to use in aircraft and other structures requiring high strength-to-weight ratios.

The stress-strain curve for this material has been determined from a previous study by Chandawanich (1) and the result shown in Figure 2.1. The specimen used to develop the stress-strain curve was pulled in uniaxial tension at a strain rate of 0.0267 in./in. per minute. Foil gages were applied to measure the strain. The tensile strengths of the 7075-T6 aluminum were found to be:

Yield strength (0.2% offset)	73.0 ksi (5.0×10^8 Pascals)
Ultimate strength	76.5 ksi (5.3×10^8 Pascals)

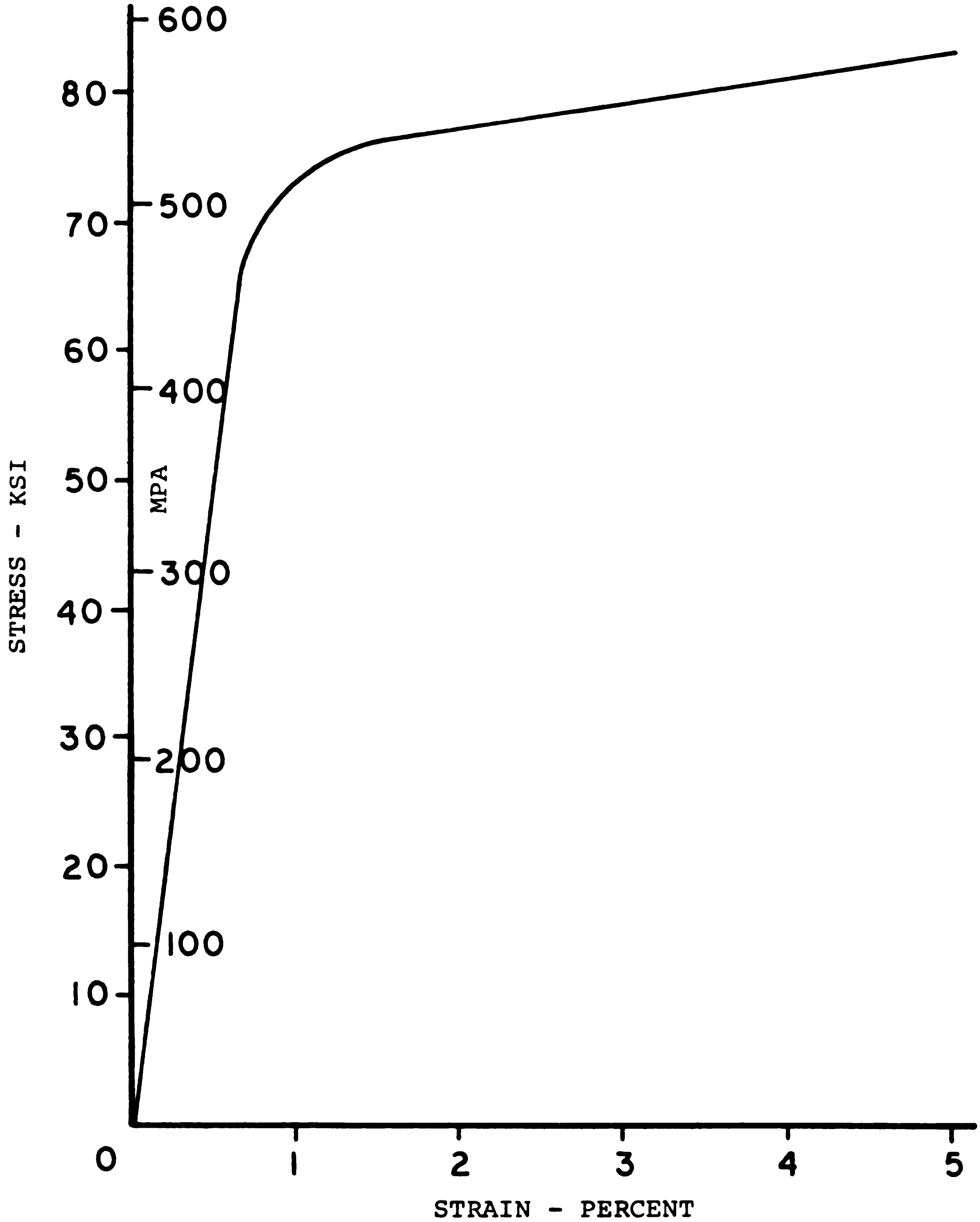

Figure 2.1 Stress-strain curve for the test specimen of 7075-T6 aluminum.

2.1.2 Specimen Preparation

The dimensions for the specimens used in this investigation are shown in Figure 2.2. Tolerances on the hole were maintained by the machine shop in order to produce, round, nontapered holes. The rolling direction of the aluminum test specimens was directed parallel to the load.

The machining process for the holes involved first drilling with a 0.1875 inch (4.76mm) drill and then honing the holes to enlarge them to a nominal diameter of 0.195 $\pm$ 0.002 inches (4.953 $\pm$ 0.051mm). Honing produced square edges around the perimeter and straight sides in the walls of the hole. The diameter was checked with a "go" - "no go" plug gage. The "go" cylinder was 0.1948 inches (4.948mm) and the "no go" cylinder was 0.1952 inches (4.958mm).

After the specimens were finished in the machine shop the hole diameters were measured at 45° intervals with a microscope equipped with an x-y stage. Since the accuracy of the diametrial measurement depended on how well the edges of the holes were located using the microscope, measurements were repeated at least three times. The variation in the repeated measurement was usually less than 0.0003 inches (8 microns). The diameters for the different specimens are shown in Table 2.1. It can be seen from this chart that the hole diameter varied from 0.1976 inches (5.02mm) to 0.1951 inches (4.96mm).

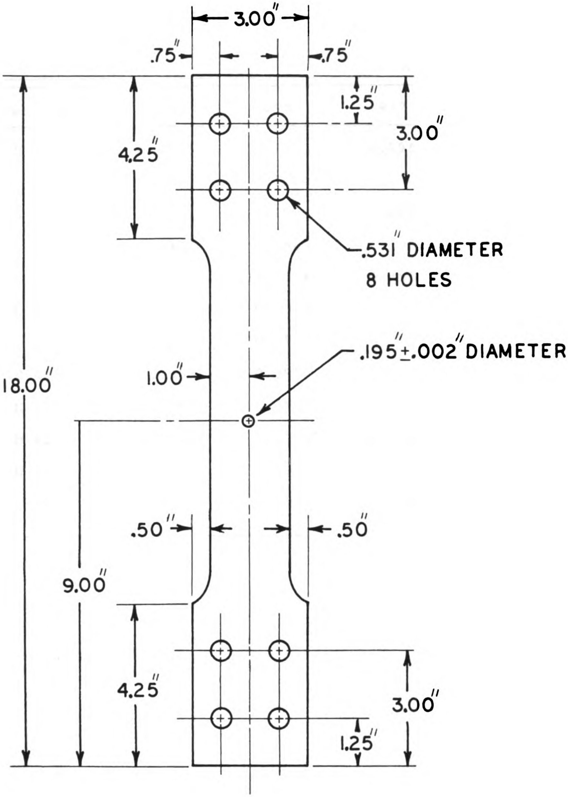

Figure 2.2 Dimensions of the test specimen.

Table 2.1 Original Diameter of Holes (in inches) for the Specimens

Specimen	0°	45°	90°	135°
N 33	0.1955	0.1955	0.1951	0.1951
N 34	0.1969	0.1964	0.1961	0.1967
N 35	0.1959	0.1958	0.1955	0.1960
N 36	0.1976	0.1969	0.1962	0.1959
N 37	0.1956	0.1954	0.1958	0.1953
N 38	0.1957	0.1964	0.1960	0.1959
N 39	0.1961	0.1957	0.1957	0.1955
N 40	0.1957	0.1957	0.1959	0.1959
N 41	0.1958	0.1957	0.1967	0.1959
N 42	0.1957	0.1960	0.1963	0.1960
N 43	0.1957	0.1955	0.1958	0.1956
N 44	0.1962	0.1959	0.1964	0.1963

The next step in preparing the specimens for testing was to apply a pattern to the surface. This technique is described in Section 3.1.4. Since the objective of this investigation is to determine the effect of coldworking on crack growth and not on crack initiation, the specimens were precracked in the uncoldworked state. The precracked length was approximately 0.04 inches (1mm) and precracking was performed on an MTS hydraulic testing machine. A detailed account of the crack growth and precrack conditions is given in Chapter 4.

Mandrelization of the precracked holes then took place followed by observation of crack growth during cycling. Mandrelization is a coldworking technique accomplished by drawing a tapered mandrel through a hole which is smaller in diameter than the mandrel. To prevent damage to the hole sides during this process, a sleeve is commonly used to line the hole. A diagram of the coldworking process is shown in Figure 2.3.

The mandrels used were part numbers JK 6540-06-188 to 192 and the corresponding diameters were 0.188, 0.190 and 0.192 inches (4.775, 4.826 and 4.877mm). A photograph of a mandrel along with a sleeve is shown in Figure 2.4. The different size mandrels allowed one to achieve a "medium coldworked" hole, which was defined to be between 0.0035 in. and 0.0041 in. (0.089mm and 0.104mm) radial expansion.

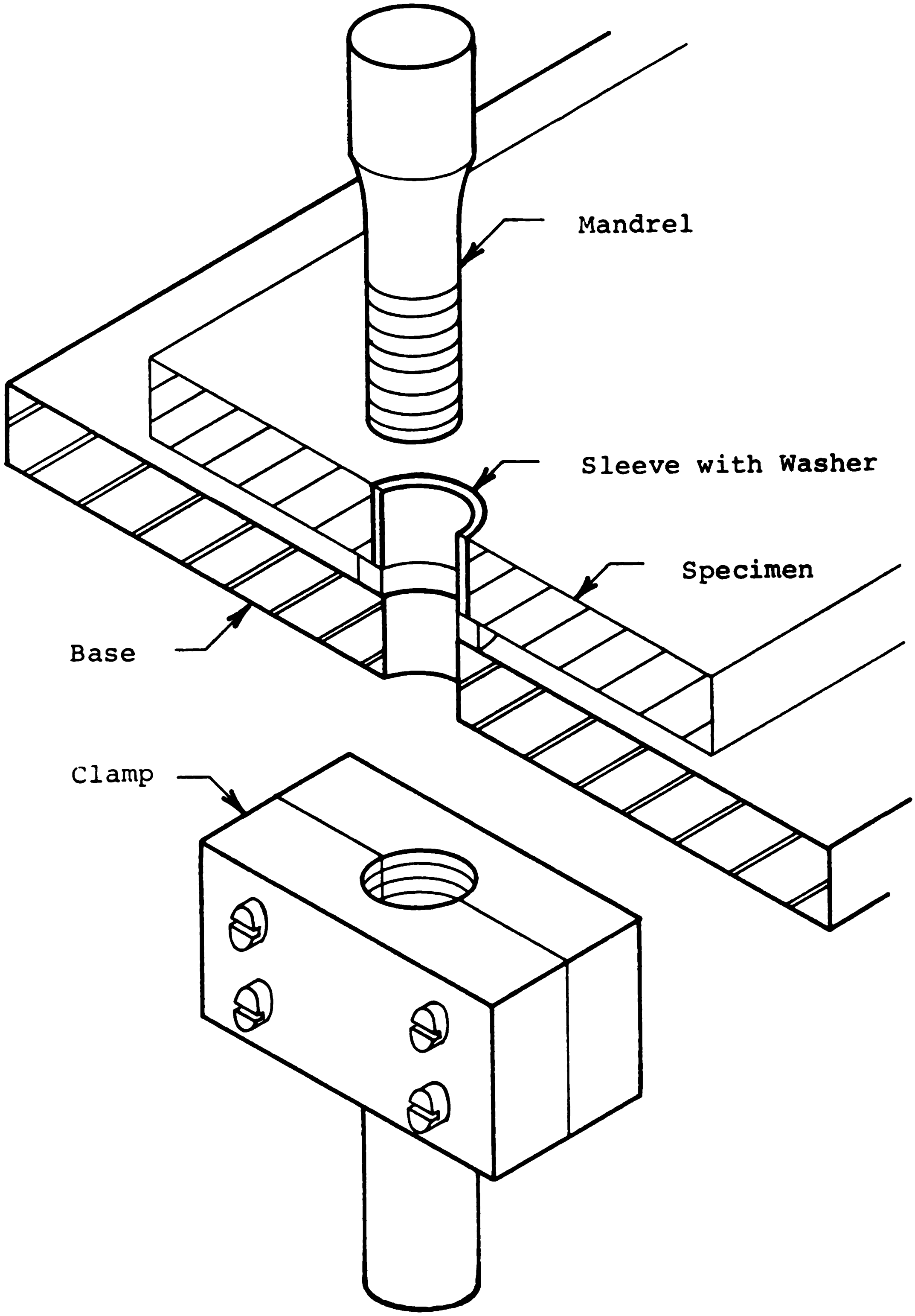

Figure 2.3 Schematic of the King coldworking process.

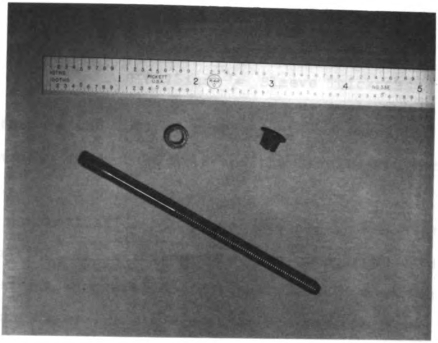

Figure 2.4 Photograph of mandrel, sleeve, and washer.

The radial expansion for a particular hole can be found by the equation:

$$\text{Radial Expansion} = 1/2\ (M - D) + 0.0075\text{inch}$$

Where: M = Mandrel Diameter

D = Hole Diameter

0.0075inch = Sleeve Thickness

The above formula was applied to the test specimens to achieve a medium coldworked hole and the results are shown in Table 2.2.

After mandrelization the protective sleeve was expanded, producing a tight fit with the hole. To remove the sleeve the specimen was supported so that the protective washer, and hence the sleeve, was not resting against the base plate. This was accomplished by placing the protective washer inside a larger thicker washer. The specimen was then mandrelized a second time, pulling out the sleeve.

A hand operated hydraulic cylinder was attached to the mandrel after it was in place to pull it through the sleeve and hole. The setup is shown in Figure 2.5. The sleeves and mandrels used were from J. O. King, Inc., Atlanta, GA and the part number is JK 5535-COGNIOL. A mild steel washer was attached to the flanged end of the sleeve to protect both the sleeve and the specimen from damage during mandrelization. This sleeve would then detach after coldworking.

Table 2.2 Radial Expansion of Specimens as Calculated from Equation

Specimen	Mandrel Diameter	Radial Expansion
	inch	inch
N 34	0.188	0.00325
N 35	0.188	0.0036
N 36	0.188	0.0032
N 38	0.188	0.0035
N 39	0.188	0.0036
N 40	0.188	0.0036
N 41	0.188	0.0035
N 42	0.188	0.0035
N 43	0.188	0.0037

Figure 2.5 Photograph of the device for pulling mandrel through hole.

It was found by Sharpe (4) that the hole is not uniformly coldworked throughout its length. Greater amount of coldworking was seen to exist on the side opposite the protective washer.

CHAPTER 3

EXPERIMENTAL PROCEDURES

3.1 Moiré Technique

3.1.1 Moiré Photography

The moiré technique was the basis for all strain measurement in this investigation. The moiré effect is the broad dark lines that occur whenever a repetitive structure is overlaid with another one. Such a pattern is observed when two fine screens are overlaid or when looking through two rows of picket fence. The arrays used to produce the moiré fringes may also be a pattern of fine dots. Densities on the order of 20,000 dots per inch may be achieved but in this investigation 1000 dots per inch was chosen. The technique of applying this dot pattern to the specimen will be described in section 3.1.4. In the following discussion the two gratings or patterns used to produce the moiré fringes will be referred to as the model, or specimen grating, and the master, or reference grating.

3.1.2 Moiré Analysis of Strain

After the patterns have been chosen and placed into position the next step in moiré analysis is to establish the relation between the relative motion of the patterns and the resulting strain in the specimen. This process involves first numbering the moiré fringes consecutively, starting near the area where the strain measurement is wanted. Next, beginning from the corresponding point on the specimen, the relative displacement between specimen and master can be calculated to be,

$$U = NP \tag{3.1.1}$$

where

U = Component of displacement along a specified coordinate axis.

N = Moiré fringe order.

P = Pitch of master.

By definition

$$\varepsilon_x = \frac{\partial U}{\partial x} \tag{3.1.2}$$

But $U = NP$

So

$$\varepsilon_x = \frac{\partial NP}{\partial x} \tag{3.1.3}$$

In the general case where the pitch of the master pattern or grating is constant the above formula for strain becomes

$$\varepsilon_x = p \, \frac{\partial N}{\partial x} \tag{3.1.4}$$

The derivative of the moiré fringe order with respect to a position coordinate can be found by plotting the fringe order as a function of the position coordinate. The slope of this curve becomes the value of $\partial N/\partial x$, and when multiplied by the pitch of the master, the product becomes the value of strain at that location. Figure 3.1 illustrates the procedure schematically.

It can be seen in Figure 3.1 b that the precision of the curve, and hence the slope, of the displacement curve depends on the number of data points defining the graph. The number of data points for the curve depends on the spacing of the moiré fringes which can be altered in two ways. If the pitch of the master grating is increased the spacing between the moiré fringes decreases, allowing for more points to be plotted. An alternative method to increase the number of points is to form an initial moiré pattern and to work with the change of fringe spacing. Such a method is called pitch mismatch and is especially valuable where strain gradients are small and fringes are spaced far apart.

One approach to the pitch mismatch method is the "fictitious strain" approach. In this method the initial fringe pattern spacing is made by mismatching the pitch of the master and specimen grating. This mismatch is accounted for as a fictitious strain and can be related to the mismatch spacing by:

$$\varepsilon_m = \frac{P}{\delta_m} \qquad (3.1.5)$$

where ε_m = Initial fictitious strain.

P = Pitch of master grating.

δ_m = Fringe spacing for initial pitch mismatch.

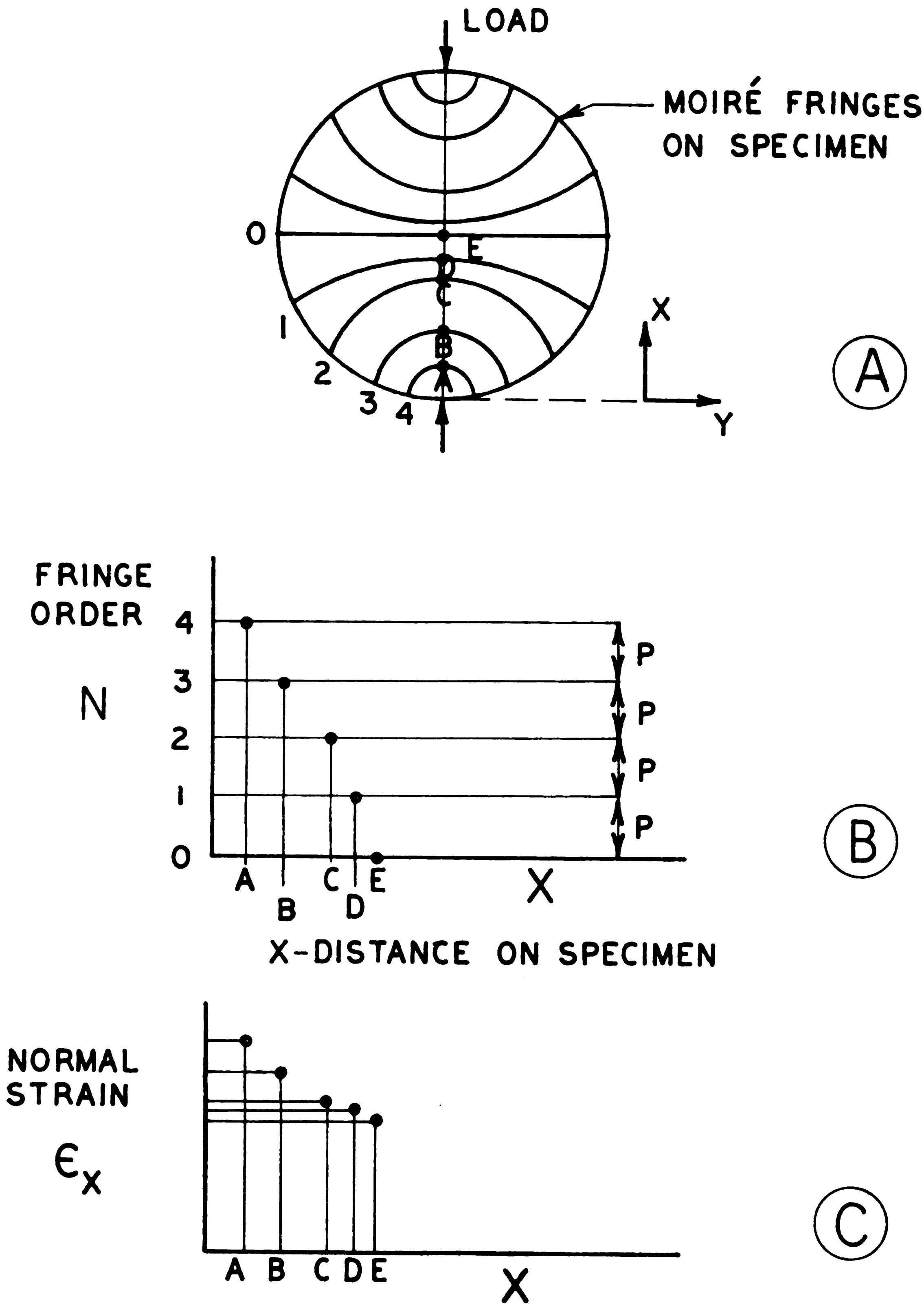

Figure 3.1 Moiré technique.

After the fictitious strain has been found, the ε_x value of strain may be found by the methods described earlier. The true strain at a desired location is now the value of ε_x at this location minus the fictitious strain, or:

$$\varepsilon_x - \varepsilon_m = \varepsilon_{true} \qquad (3.1.6)$$

In the method of pitch mismatch, the pitch of the master grating is different than that of the model grating. This mismatch may occur in cases where it was not intentional, but it still must be accounted for. Serious error will result by assuming a matched pair of gratings since a mismatch of 0.1 percent will show up as a large strain of 0.001.

3.1.3 Application of Moiré Analysis

Since in this investigation the strain in a particular direction around a coldworked hole was to be found, it is interesting to look at how the method of moiré analysis applies. The typical moiré pattern formed after coldworking a hole is shown in Figure 3.2b. From geometric considerations it is best to work in polar coordinates and therefore the radial and tangential components of strain are labeled ε_r and ε_θ respectively. These are shown in Figure 3.2c. The first step in moiré analysis is to number the fringes. A value for radial strain will be measured first so a radial line taken perpendicular to the fringes is numbered and the corresponding distances measured as shown in Figure 3.3.

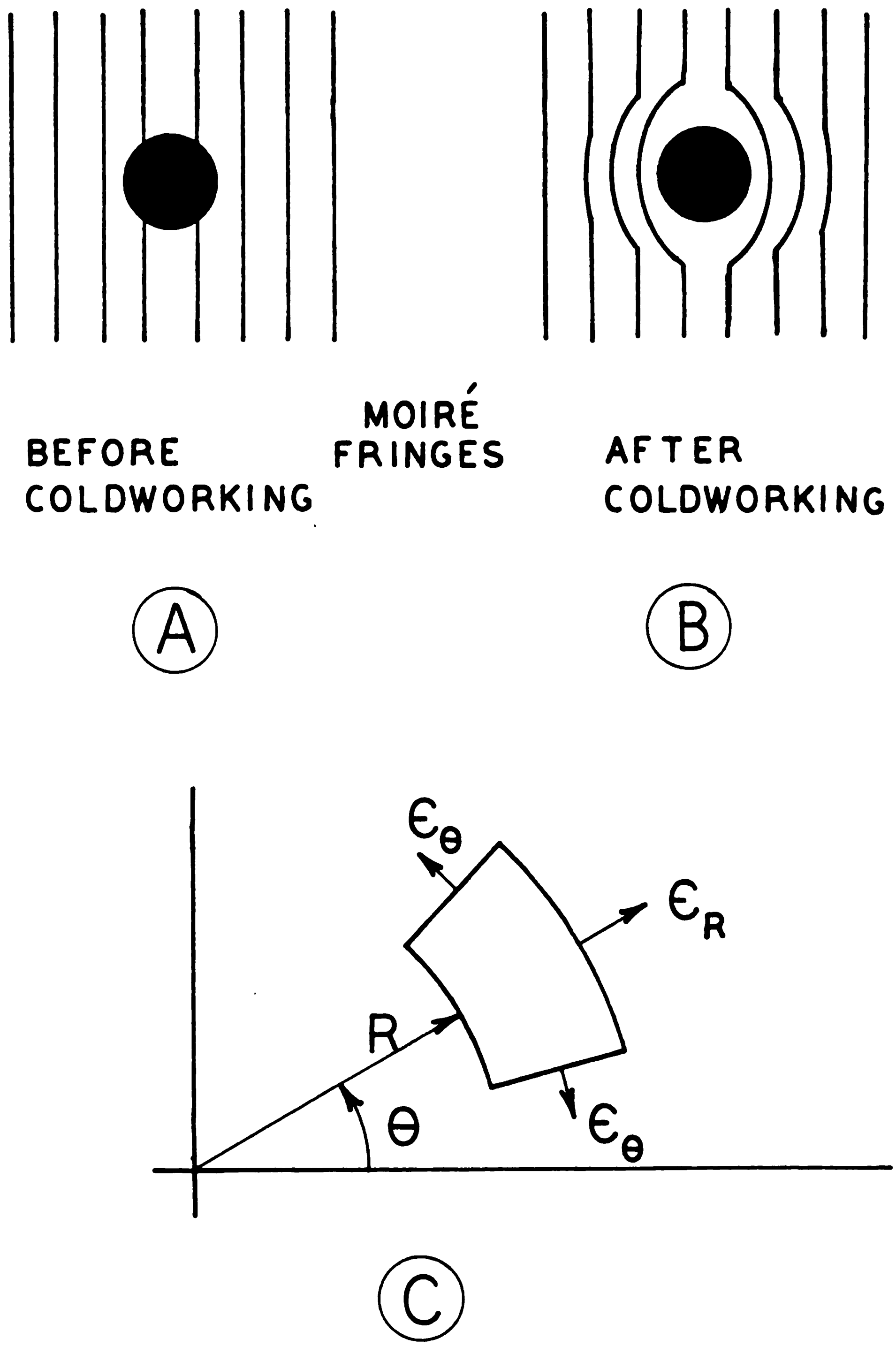

Figure 3.2 Moiré fringe around hole and a drawing of the coordinate system.

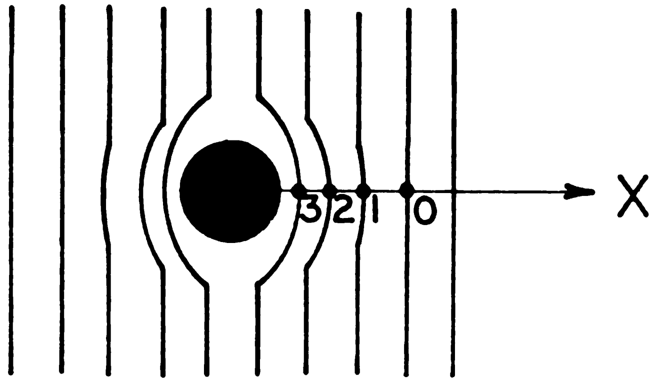

FRINGE ORDER N	DISTANCE FROM HOLE EDGE - X
0	1.1 MM
1	0.8
2	0.6
3	0.5

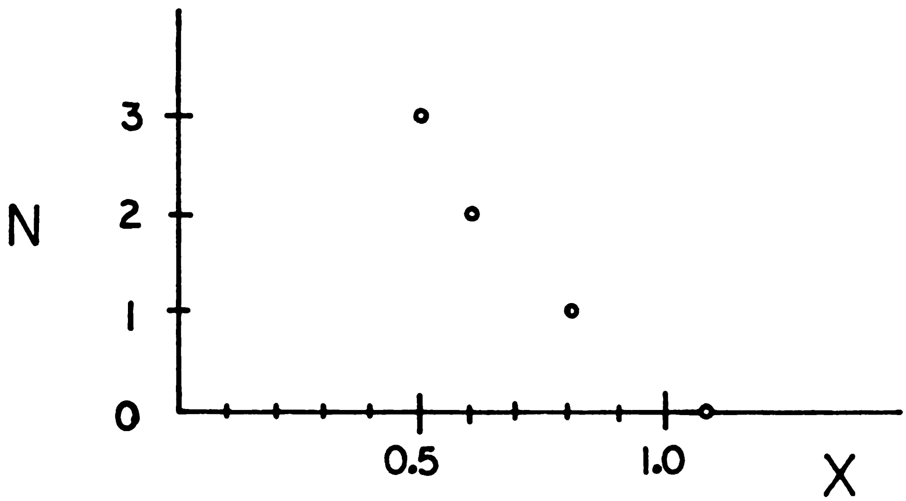

Figure 3.3 Moiré technique for radial strains.

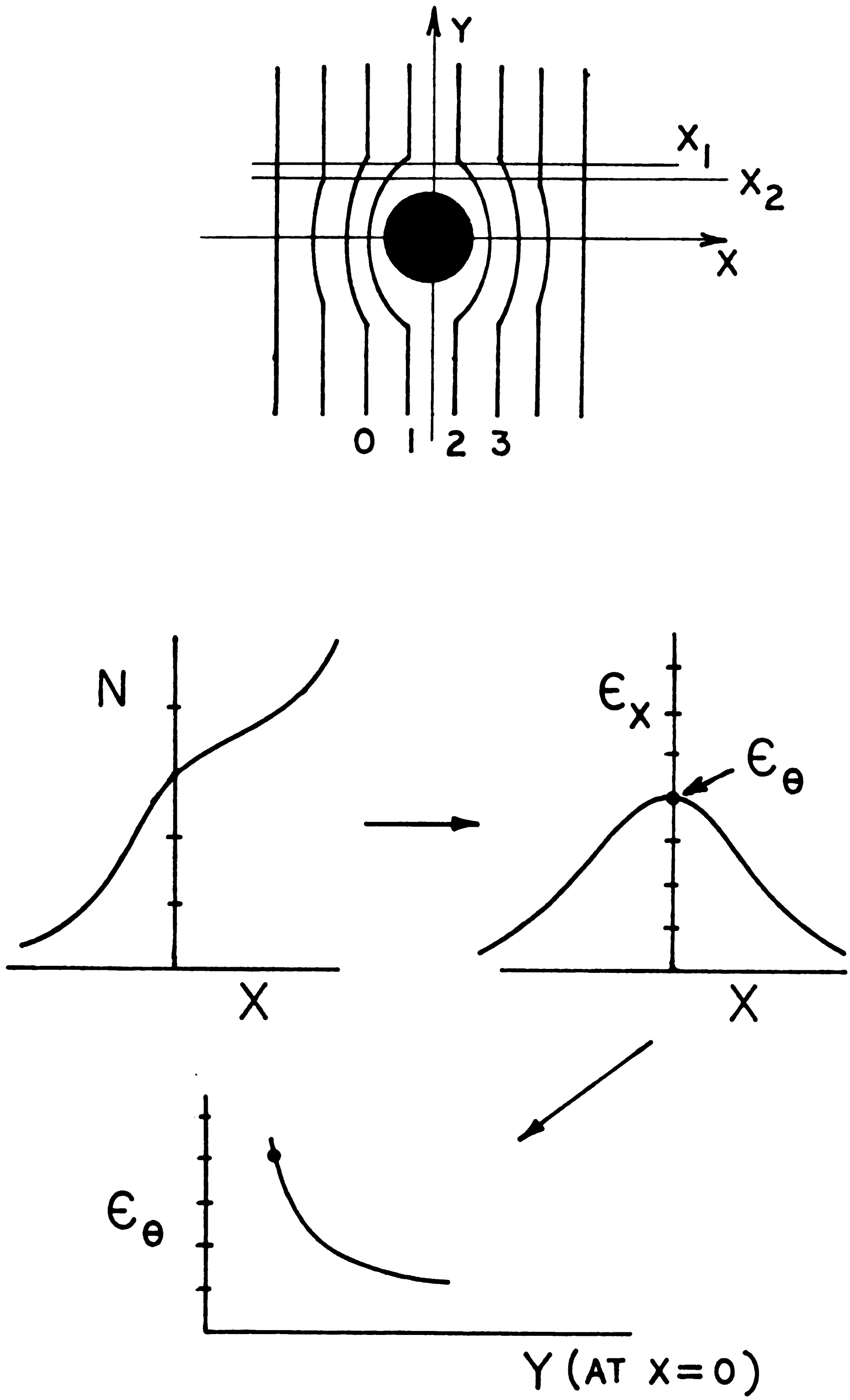

Figure 3.4 Moiré technique for tangential strains.

From this information a displacement graph is constructed, followed by calculations of the radial strains. The tangential strains may be found by an extension of the radial strain formulation. The major difference is that several lines parallel to the x direction, called x_1, x_2, ..., are used whereas in the radial strain calculation only one axis was needed. The tangential strain calculation is shown in Figure 3.4.

3.1.4 Grid Production and Printing

Since master gratings are easily damaged, a set of submasters were made to be used in producing the pattern on the specimen. The master grating used was purchased from Graticules Limited, Sovereign Way, Tonbridge, Kent, Great Britain. The set of submasters were made by contact printing on Kodak HRP plates in a parallel light field as shown in Figure 3.5. The distance between film plate and light source was 60 inches (152.4cm) and exposure time was 10 seconds.

Before printing the grid on the aluminum specimens the surface was sanded and polished to insure proper adhesion of the applied pattern and also to produce a highly reflective surface which was necessary to observe and photograph the moiré fringes. The sanding was done under running water using sandpaper grits 350, 400 and 600. Next the surface

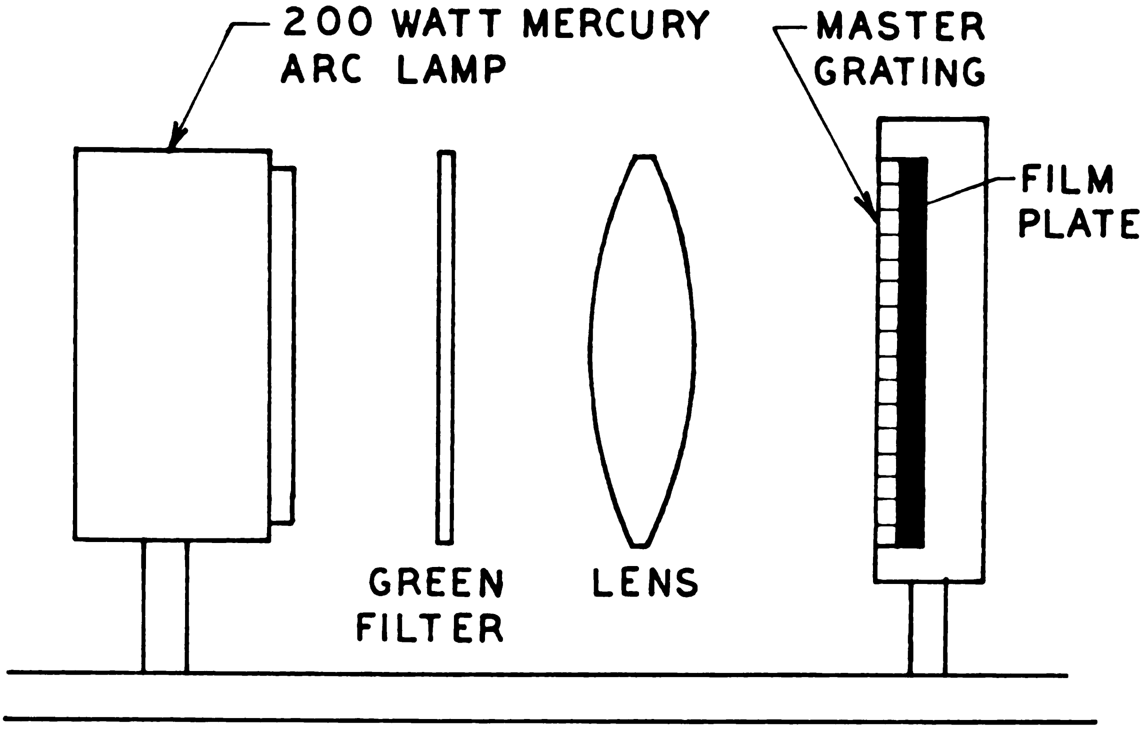

Figure3.5 Optical system for producing a submaster from a film plate.

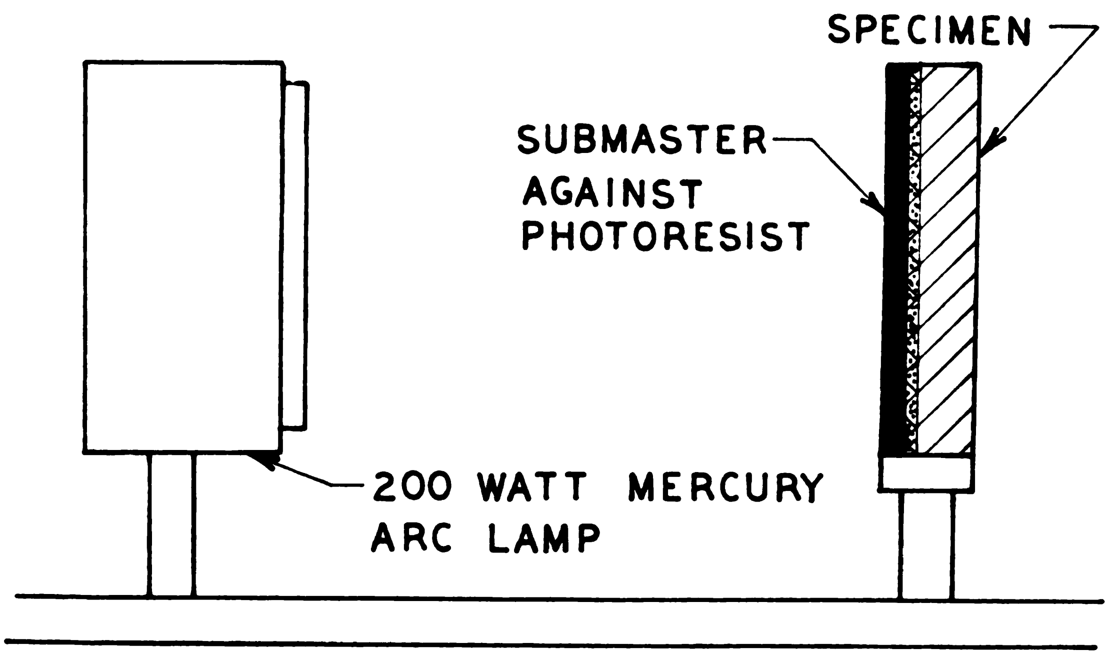

Figure 3.6 Optical system for printing a grid on specimen.

was polished with 1 micron and 0.3 micron alumia particles suspended in oil and finally degreased with acetone.

After polishing and thorough cleaning, the specimen was ready for grid application. The method of grid application used was one in which the pattern of grid was photographically printed onto the specimen surface. This was accomplished by first spraying the surface with a light-sensitive emulsion which, after drying and baking at 90°C for 20 minutes is exposed to the submaster pattern in a contact printer. When the specimen was developed and washed a photographic reproduction was left on the surface. The type of emulsion used was AZ 1350B photoresist purchased from Shipley Company, Inc., Newton, Mass. An airbrush was used to spray the photoresist which resulted in a coating thickness on the order of 0.3 to 1.0 microns and an exposure time of 3 to 4 minutes. The photoresist formed a thicker coating near the hole edge which made it difficult to obtain a dot pattern in that area. Longer exposure times and more practice in spraying helped to overcome this problem. A 200 watt mercury arc lamp was used to expose the photoresist and was placed about 16 inches (40.6cm) in front of the submaster and specimen. Figure 3.6 shows the exposure setup.

A dot pattern was chosen to be printed on the specimen in order to facilitate strain measurement in two perpendicular directions so that both ε_r and ε_θ could be measured at a given location. The dot pattern was produced by rotating the submaster 90° with respect to the specimen and exposing a second time. The results of this method are shown in Figure 3.7.

3.1.5 Moiré Optical System

In order to form moiré fringes a submaster pattern was superimposed with a specimen pattern. This superposition can be accomplished in one of two ways, mechanically or optically. The optical method was chosen because a pitch mismatch could be easily introduced which is a valuable technique for small strain gradients as explained in section 3.1.1.

The type of camera used in the optical system was a Schneider Optick Krueznach with a f 4.5 lens of 11.8 inches (300mm) focal length. This camera was mounted on a heavy table which was cushioned with rubber air bags. The purpose of the air bags was to insulate the table from building vibrations. The illumination used was a 150 watt spot light placed about 30 inches (76.2cm) from the specimen and with an angle of incidence of about 30°. The optical setup is shown in Figure 3.8. The second camera used to record the fringes was a Graflex. The type of film used was Polaroid type 57 high speed film (3000 ASA). This type of film was needed because of the low lighting conditions.

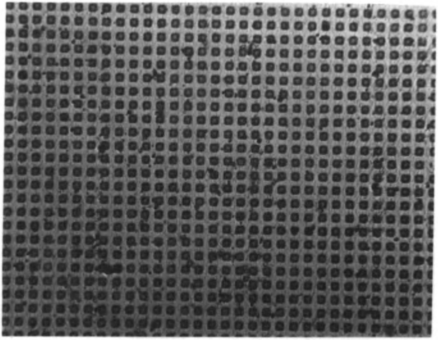

a) Photograph of dot pattern.
Magnification x150

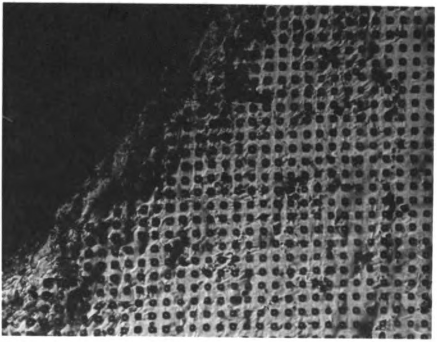

b) Dot pattern around coldworked hole.
Magnification x150

Figure 3.7

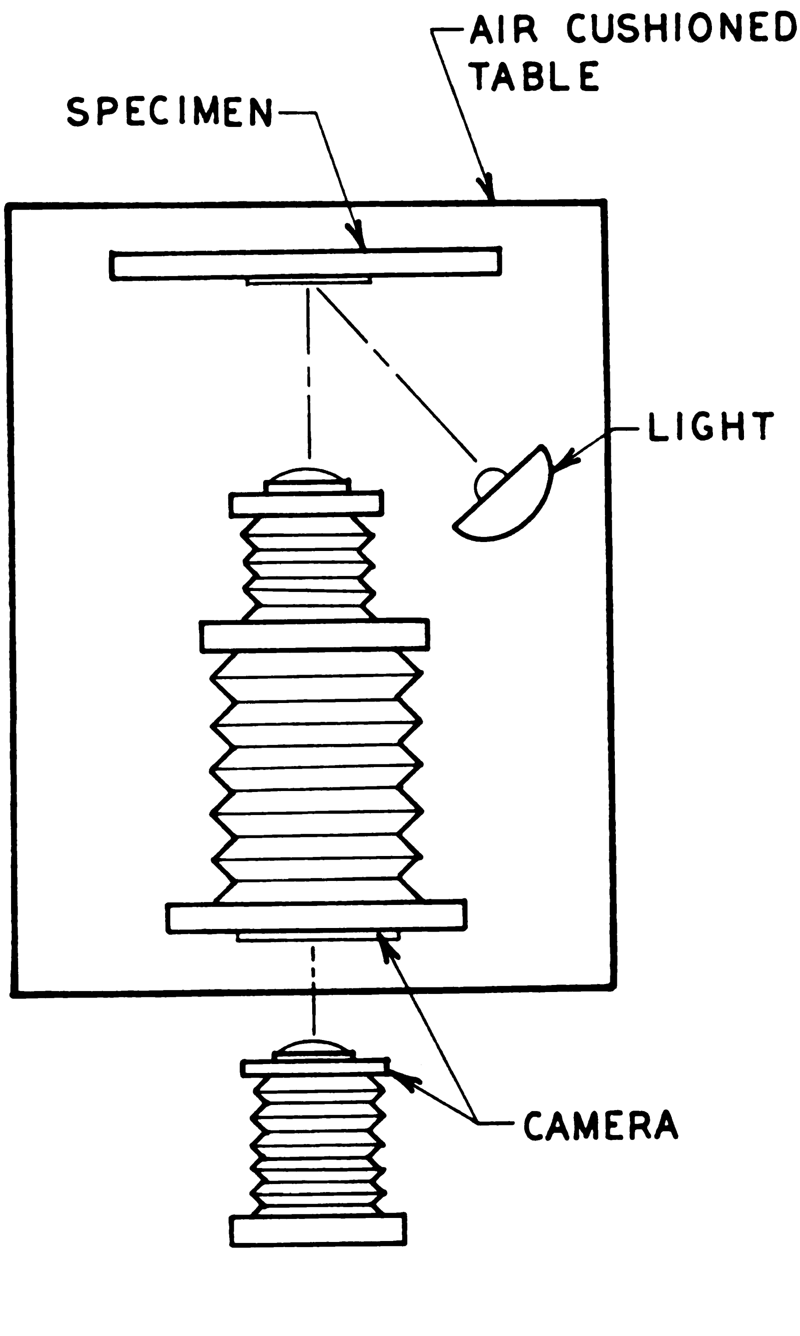

Figure 3.8 Top view of optical system for moiré photography.

This optical system was then used to create a real image of the specimen pattern in a plane containing the master or submaster which was located in the film plane of the first camera. Both the specimen pattern and the submaster pattern were of the same spacial frequency, 1000 lines per inch. Pitch mismatch can be introduced by magnifying the specimen pattern and then projecting it onto the submaster. A magnification of 3 was used which resulted in a 333 line per inch specimen pattern projected onto a 1000 line per inch submaster. The resulting mismatch was photographed and can be seen in Figure 3.9. This setup was then used to photograph the moiré fringes of the mandrelized specimens from which the strains were calculated; see Figure 3.9.

3.2 Interferometric Displacement Gage (IDG)

The IDG technique has been used in this investigation for experimental calculation of the stress intensity factor. The stress intensity factor, K, is given by the following relation:

$$K = \sigma\sqrt{\pi a} \quad F(a) \tag{3.2.1}$$

where σ = Remote load.

a = Crack length.

$F(a)$ = Flaw geometry.

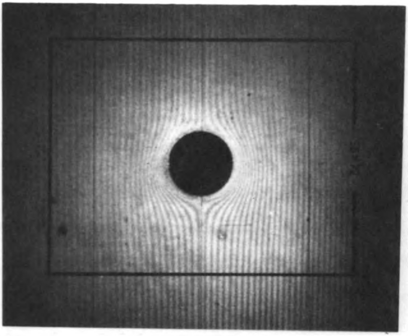

Figure 3.9 Real time moiré fringe pattern with initial mismatch for residual coldworked specimen. Magnification 3:1

The K value characterizes crack behavior in many materials and has the units of stress times the square root of length. The calculation of this value begins with consideration of the components of displacement at a point near the crack tip for mode I loading and plane stress conditions.

$$U_x = \frac{K_1}{G}\sqrt{\frac{r}{2\pi}} \cos\frac{\theta}{2} \left[\frac{1-\nu}{1+\nu} + \sin^2\frac{\theta}{2}\right] \qquad (3.2.2)$$

$$U_y = \frac{K_1}{G}\sqrt{\frac{r}{2\pi}} \sin\frac{\theta}{2} \left[\frac{2}{1+\nu} - \cos^2\frac{\theta}{2}\right] \qquad (3.2.3)$$

where

U_x, U_y $\equiv$ x and y components of displacement

G $\equiv$ Shear modulus

ν $\equiv$ Poisson's ratio

Combining equations 3.2.1 and 3.2.3 and solving for F(a), one obtains

$$F(a) = \frac{G\sqrt{\frac{2}{\nu a}}\ {U_y}/{\sigma}}{\sin\frac{\theta}{2}\left[\frac{2}{1+\nu} - \cos^2\frac{\theta}{2}\right]} \qquad (3.2.4)$$

Using equation 3.2.1 again and substituting in the result for the flaw geometry gives,

$$K = \sigma\sqrt{\pi a}\ \frac{G\sqrt{\frac{2}{\nu a}}\ {U_y}/{\sigma}}{\sin\frac{\theta}{2}\left[\frac{2}{1+\nu} - \cos^2\frac{\theta}{2}\right]} \qquad (3.2.5)$$

All the terms on the right side of equation 3.2.5 can either be found from load and geometry (σ), crack geometry (a,r,θ), or material properties (ν,G), except for the value of U_y. This component of displacement may be found by using the IDG technique, but it is more convenient to find the ratio U_y/σ. Once this ratio has been determined the value for the stress intensity factor, K, can be determined for a particular cracklength. The method of the IDG technique and how it was used to determine U_y/σ is described next.

3.2.1 Basics of the IDG

The principal of the interferometric displacement gage developed by Sharpe (5) is based on the interference pattern produced when coherent light is directed toward two indentations (see Figure 3.12). These indentations are pyramidal in shape and are pressed into a specimen's surface spanning a crack as shown in Figure 3.10. As the specimen is loaded the crack will open causing a change in the distance, D, between the indentations. This displacement in turn causes a motion of the fringes in the interference pattern. The purpose of the interferometric displacement gage is to relate the fringe movement with the crack opening. This relationship was aided by the use of computer techniques. The input information to the computer was the fringe data and with the proper program the data was converted to the crack opening displacement. This output was then channeled to an X-Y recorder and the displacement plotted on the X-axis while at the same time the Y-axis of the recorder monitored

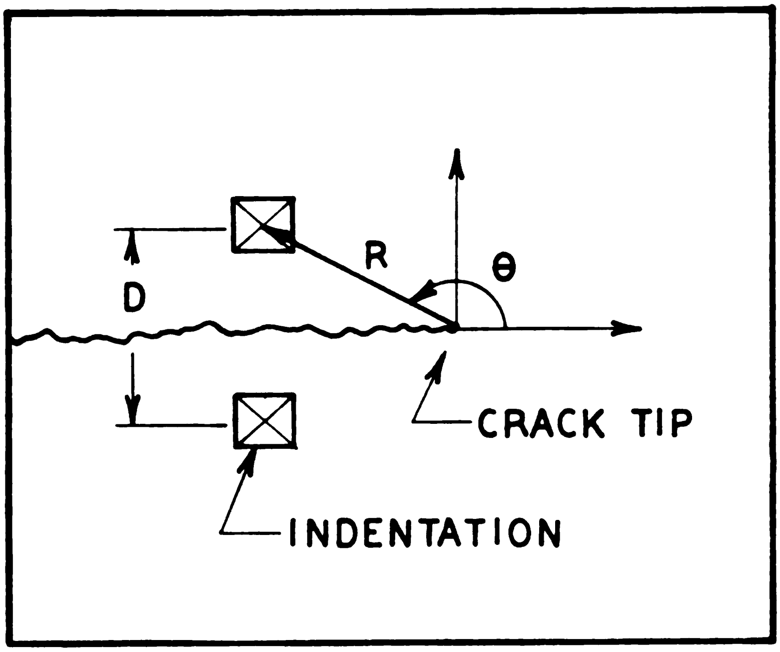

Figure 3.10 Drawing of a fatigue crack defining the crack tip coordinates and showing surface indentations.

the applied load to the specimen through a load cell. A typical load displacement curve drawn by the X-Y recorder is shown in Figure 3.11 along with the experiment setup. The slope of this load displacement curve was the final value needed to calculate the stress intensity factor, K, in equation 3.2.5. The following discussion describes the relationship mentioned earlier between the fringe motion and crack opening displacement.

The mathematical relationship between the indentation spacing and the fringe order is

6) $$d \sin \alpha_o = m\lambda \qquad (3.2.6)$$

where $d \equiv$ Indentation spacing.

$\alpha_o \equiv$ The angle between the incident and reflected beams.

$m \equiv$ Fringe order.

$\lambda \equiv$ Wavelength of the incident beam.

From the above equation it can be seen that the change in indentation spacing, δd, can be related to the change in fringe orders, δm, at a fixed observation point by the following equation:

7) $$\delta d = \frac{\delta m \ \lambda}{\sin \alpha_o} \qquad (3.2.7)$$

Fringe motion may also be caused by a rigid body motion as well as a relative displacement of the two indentations.

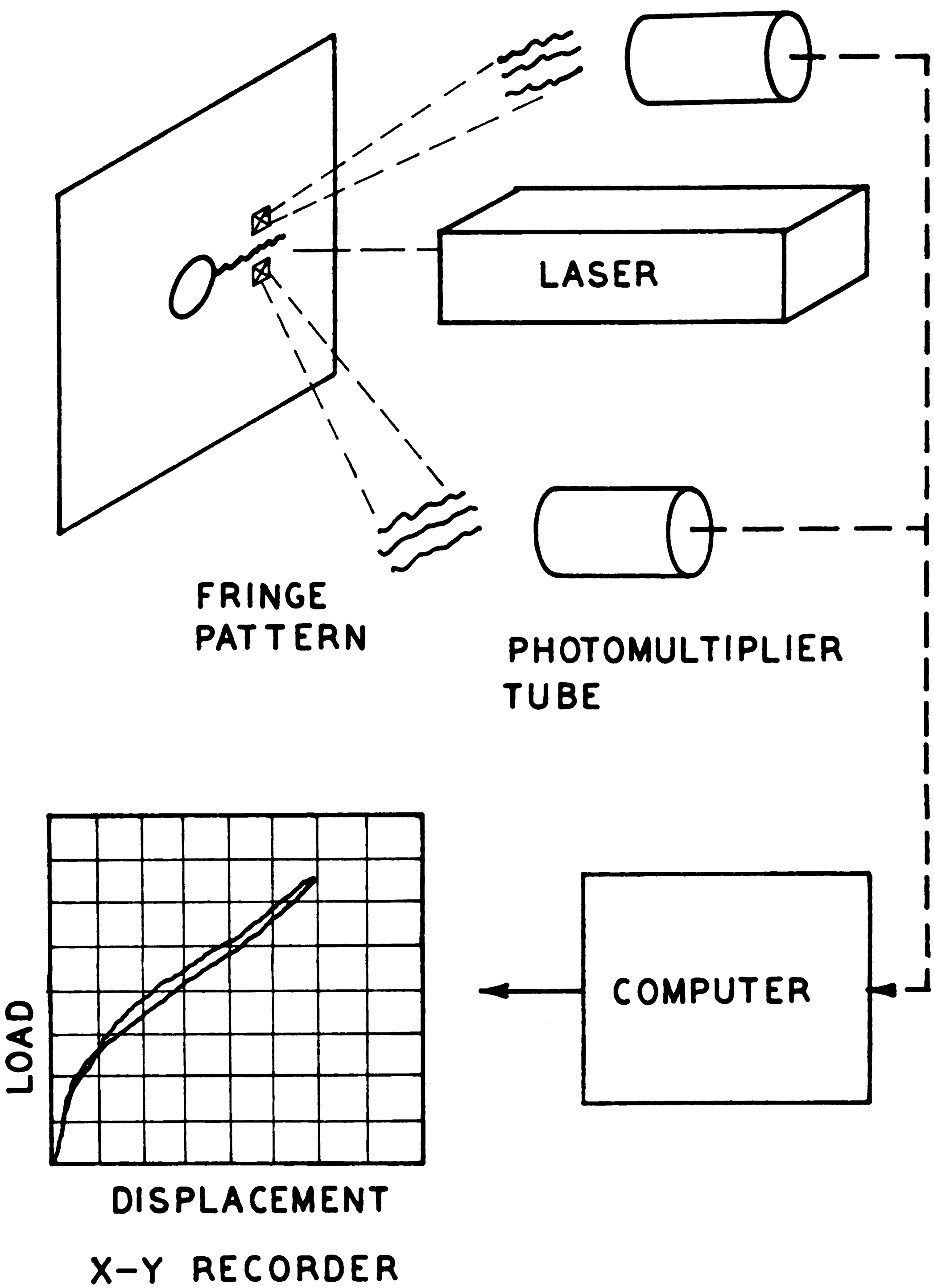

Figure 3.11 Schematic of the IDG and computer setup.

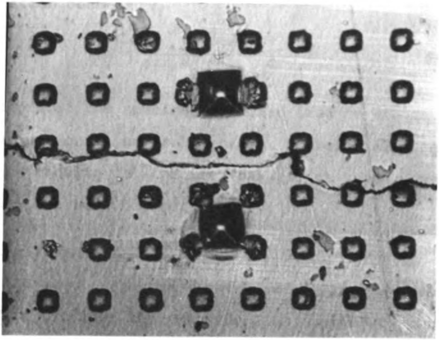

Figure 3.12 Photograph of a pair of indentations and dot pattern on specimen. Magnification X560.

When a specimen moves in its plane and along a line between the indentations, one fringe pattern moves toward the incident beam, and one moves away. The fringe motions are therefore average to eliminate the rigid body motion. The above equation becomes:

$$\delta d = \frac{\lambda}{\sin \alpha_o} \quad \frac{\delta m_1 + \delta m_2}{2} \qquad (3.2.8)$$

Other motions of the specimen can also lead to errors such as one perpendicular to the specimen. Careful alignment of the testing machine and specimen can reduce these movements, eliminating the need for corrections.

3.2.2 Displacement Measuring Instrument

The IDG uses a Spectra Physics model 120 5 MW He-Ne laser. This provides the coherent light necessary for the fringe pattern generation. Two photomultiplier tubes were used to sense the fringe motion and convert it to an electrical signal. These were mounted approximately 17 cm from the indentations on the specimen. The electrical signal was then channeled to a minicomputer system which processed the fringe movement data and plotted the resulting crack opening displacement on an X-Y recorder. Description of the system is given in Reference 6.

3.3 Servocontrolled Testing Machine

To apply the fatigue cycles to the aluminum test specimens a servocontrolled closed-loop hydraulic testing machine was used. The testing machine was manufactured by MTS Systems Corporation and consisted of a hydraulic power supply model 506.02, an actuator (servoram) model 204.63, a load frame model 312.21, an electronic control panel model 406.11, and a function generator model 410. The load to the specimen was determined from a load cell model 661.21A-03. The machines dynamic rating is ± 20 kips (89000N).

The control console consisted of a servocontroller, a control unit, a function generator, a cycle counter, and a transducer output signal. The purpose of the console is to control the motion of the actuator which is connected to a hydraulic power supply through a servovalve. This servovalve opens or closes according to the control signal from the servocontroller. The servocontroller receives its information from the function generator which is programmed by the operator. The servocontroller has an error detector circuit that can open a failsafe interlock to stop the test if an error between the command and feedback signal exceeds a preset limit. The output signal is monitored by both a digital voltmeter and an oscilloscope. Figure 3.13 shows a photograph of the equipment used.

Figure 3.13 Equipment used in fatigue testing.

The specimens in this investigation were loaded with a Haversine waveform with a constant amplitude and having a maximum value of 7500 lbs (33375 N) and a minimum value of 750 lbs (3337.5 N). The frequency of the waveform was 15 Hz. The rolling direction of the aluminum test specimens was directed parallel to the load and the test was performed at room temperature (70-75°F).

4.

cc

ti

cf

cr

cr

ev

in

fo

cr

wi

an

4.

co

on

sho

sam

CHAPTER 4

CRACK GROWTH

4.1 Overview

Cracks usually initiate at points of maximum stress concentration such as holes, fillets, keyways, and unintentional stress raisers such as tool marks or burrs. The life of structural components that contain cracks or that develop cracks early in their life may be governed by the rate of crack propagation.

It is the purpose of this part of the investigation to evaluate how well a mandrelization process works in extending the fatigue life of a specimen when a crack has already formed. One way to perform this evaluation is to study the crack growth data. Included in this Chapter is a comparison with the work of Chandawanich (1), whose specimen dimensions and fatigue procedure were duplicated.

4.2 Experimental Results

Crack lengths were measured on both surfaces of the coldworked specimens. It was found that the crack lengths on the back side (the side supported when coldworked) were shorter than the crack lengths on the front side after the same number of cycles. This was due to a difference in the

amo
whi
pro
dra
hol
ed
rea
str
hav

ing
ler
In
hol
des
sp

va
le
cy
Ch
fr
Fi

amount of residual strains between the front and back side which was developed during coldworking (4). The coldworking process exerted a force perpendicular to the specimen by drawing a tapered mandrel through a sleeve inserted into the hole. The sleeve was flanged on the side which was supported to prevent it from slipping out during mandrelizing. The reaction of both the flange and the sleeve acted to constrain deformation of the hole on the back side which may have lead to the reduction in crack growth.

Several cracks appeared around the coldworked hole during cycling but just one crack continued to grow to the length of 6mm for each specimen, see Figures 4.1 to 4.6. In two specimens, N 36 and N 38, the sleeves inserted into the hole were left in after the coldworking process. These are designated by the word sleeve which appears next to the specimen number.

The number of cycles necessary to grow a crack to 6mm varied with each specimen; for example, in specimen N 34 less than 50,000 cycles were needed compared to 400,000 cycles in specimen N 43. This variation did not occur in Chandawanich's data (1) and a typical crack growth curve from his report is compared to the data in this report in Figure 4.7.

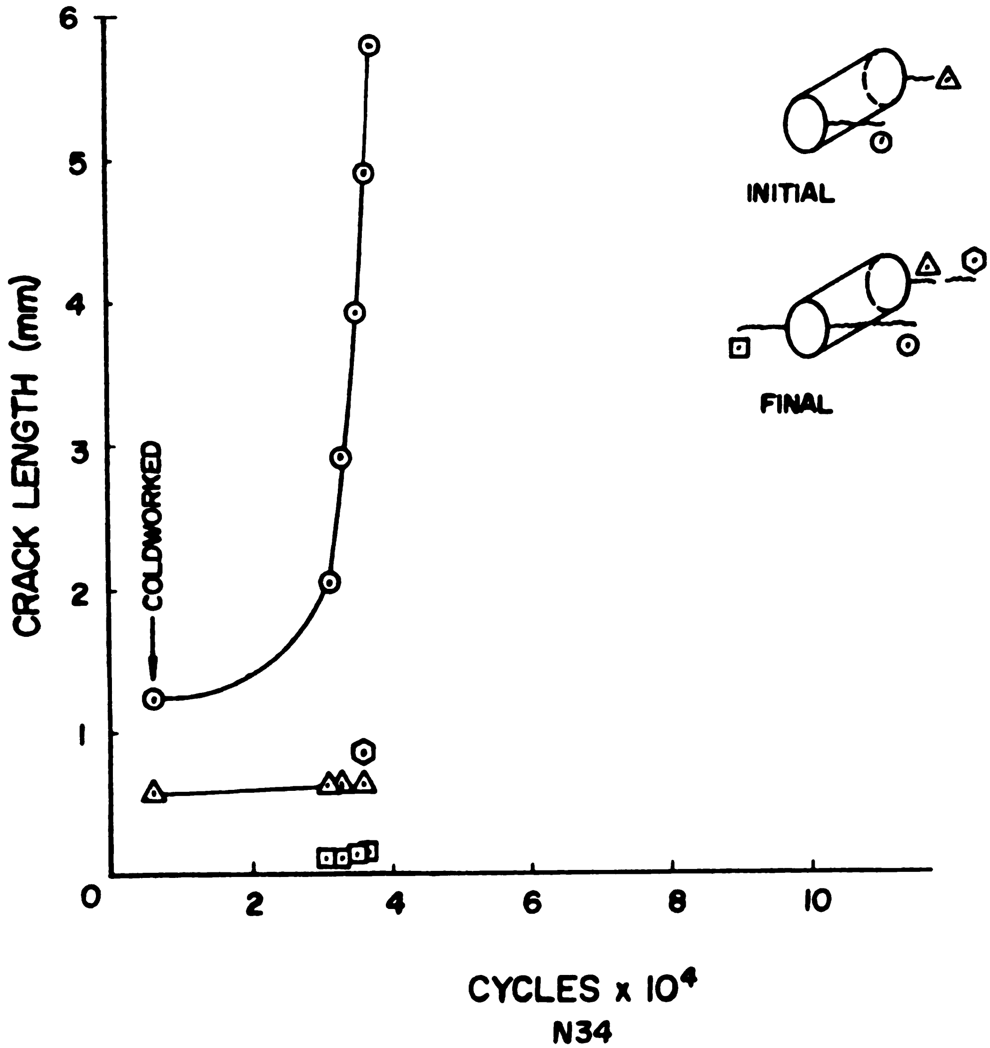

Figure 4.1 Crack growth data for specimen N 34 (medium coldworked).

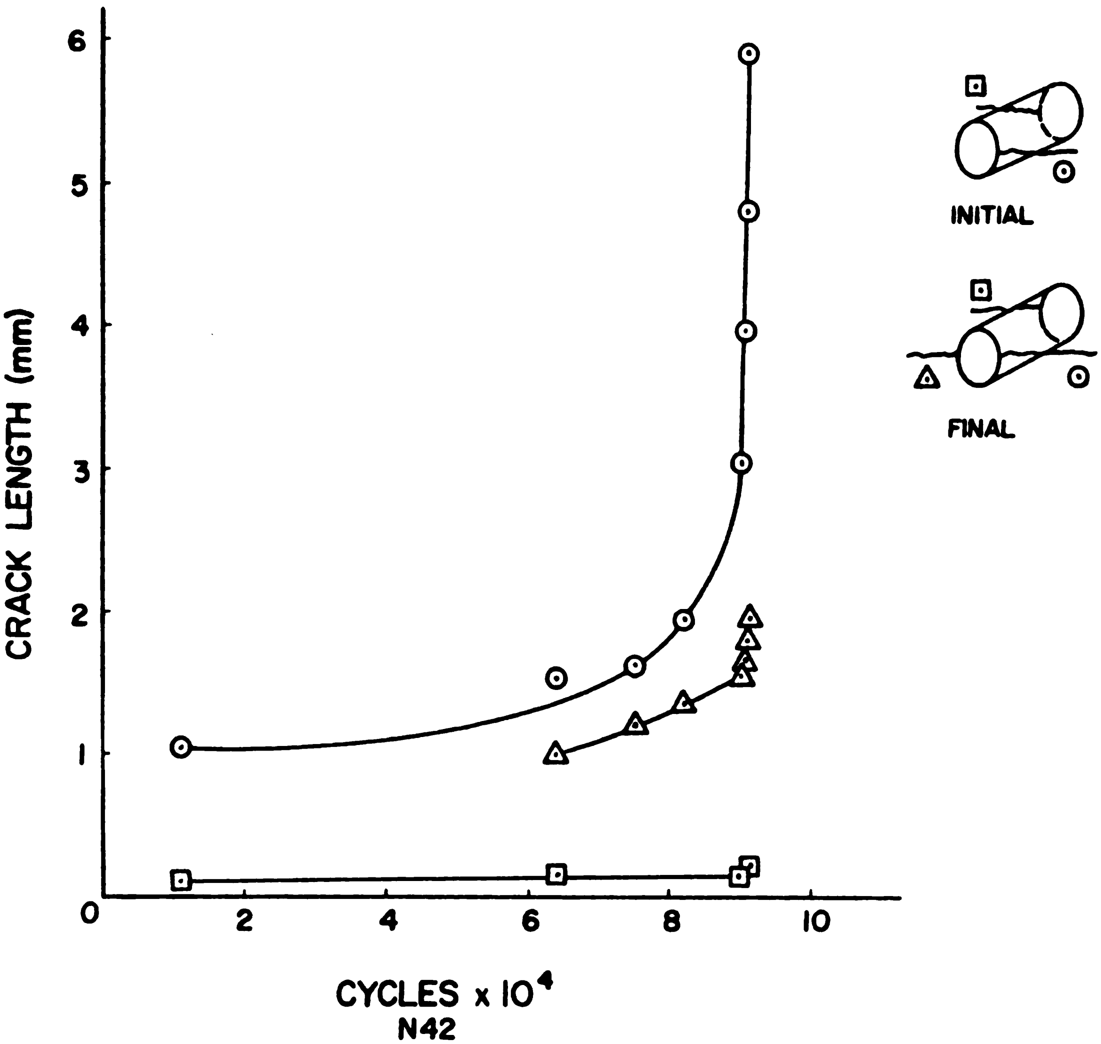

Figure 4.2 Crack growth data for specimen N 42 (medium coldworked).

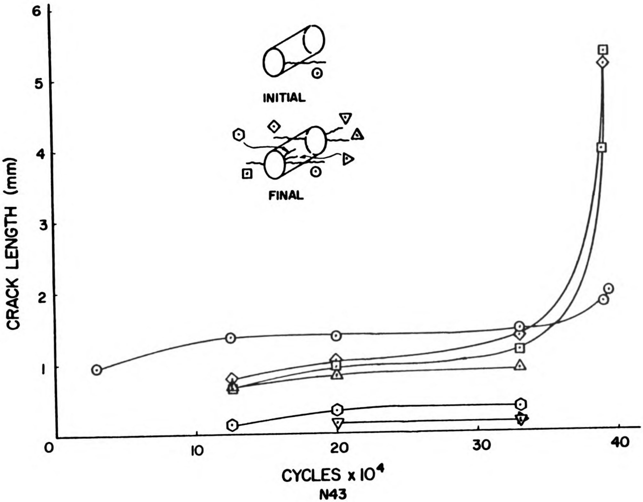

Figure 4.3 Crack growth data for specimen N 43 (medium coldworked).

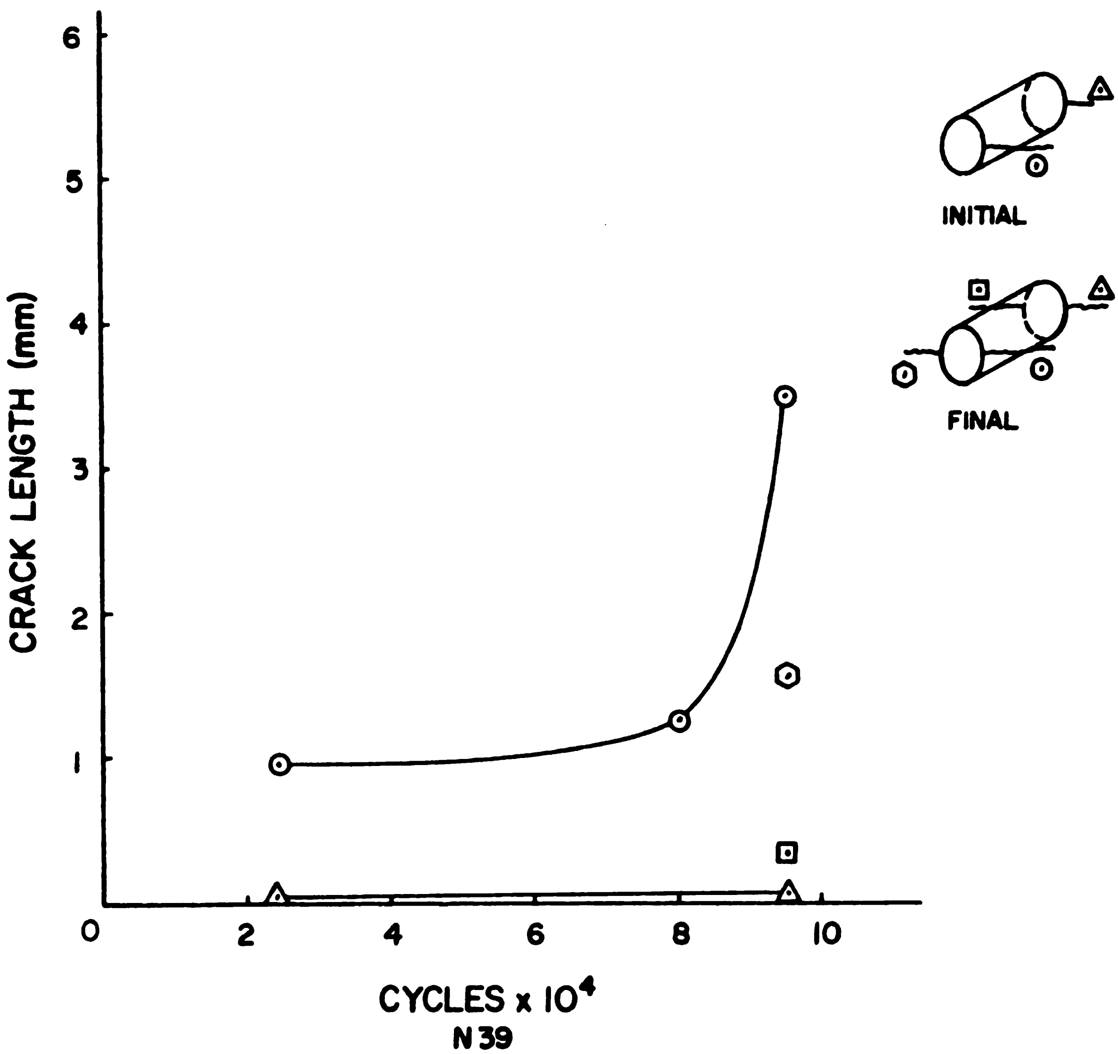

Figure 4.4 Crack growth data for specimen N 39 (medium coldworked).

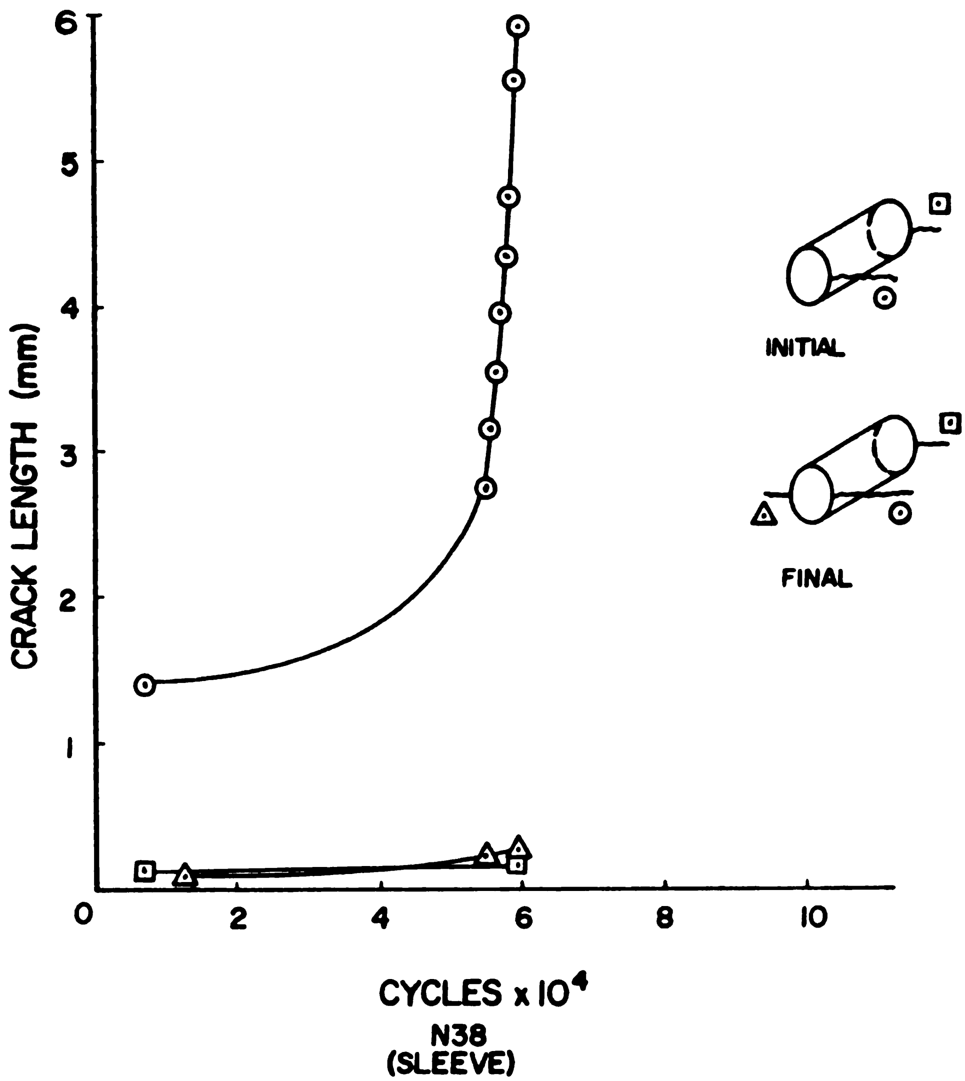

Figure 4.5 Crack growth data for specimen N 38 with sleeve (medium coldworked).

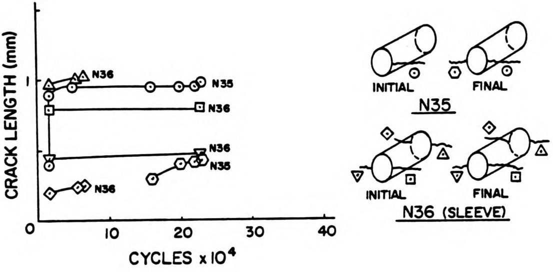

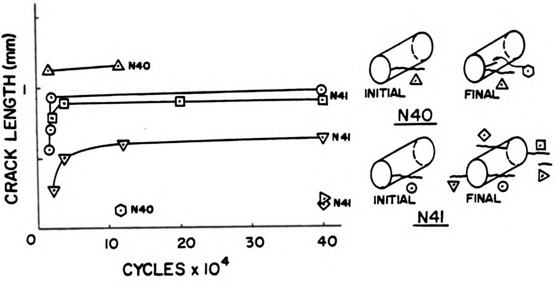

Figure 4.6 Crack growth data for specimens N 35, N 36 with sleeve, N 40 and N 41 (medium coldworked).

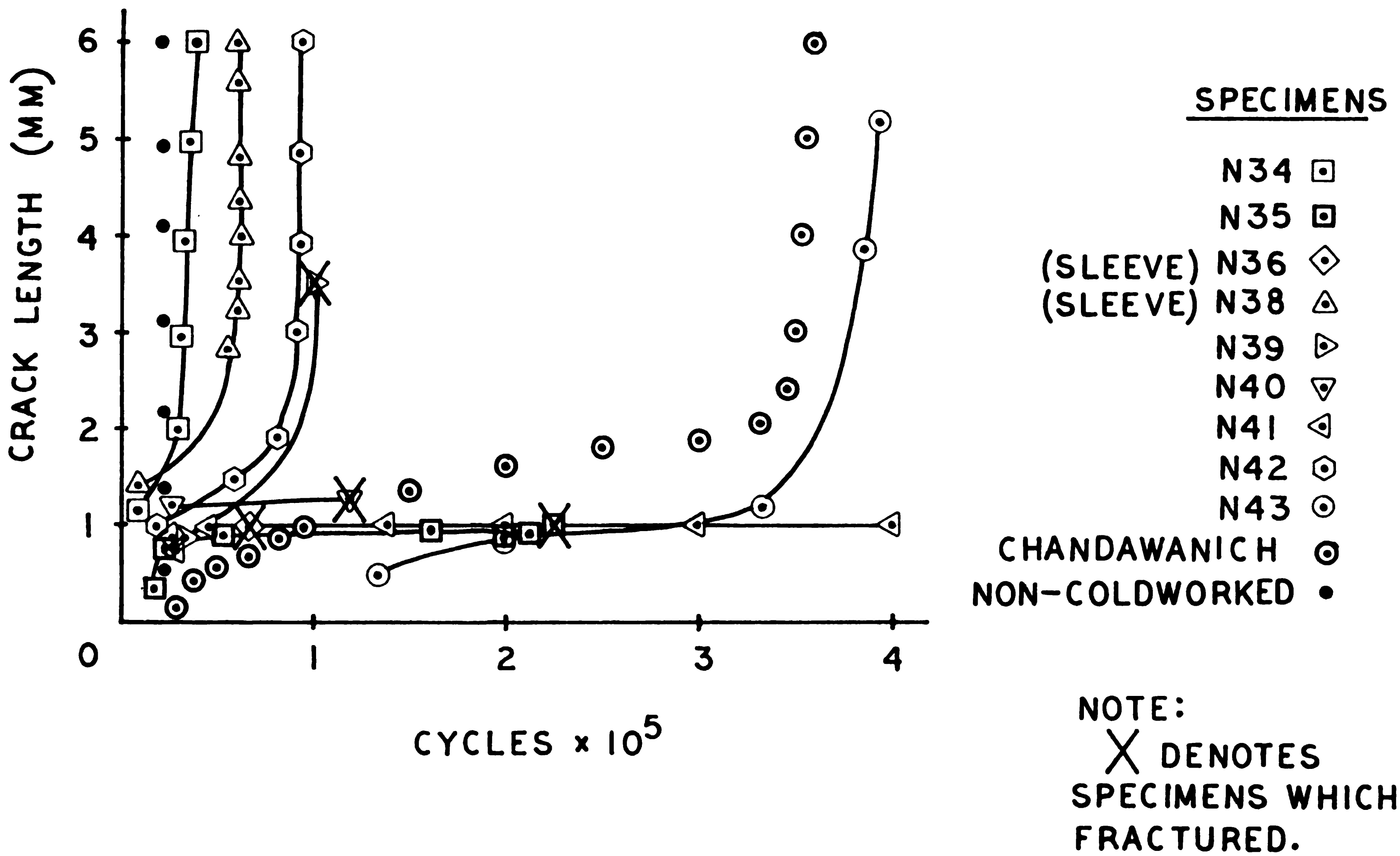

Figure 4.7 Crack growth data.

4.3 Discussion of Results

The effect of the sleeve on crack growth can be seen in Figure 4.7 for specimens N 36 and N 38. Specimen N 36 fractured in a relatively few number of cycles so the effect of the sleeves can not be determined from this specimen. Specimen N 38 did not fracture and its crack growth curve indicates the sleeve had no effect on the number of cycles to grow the crack to 6 mm.

Four fractures occurred out of the nine specimens tested. One of these fractures was due to a loose clamp and caused excessive stress at one of the bolt holes which held the specimen. Another fracture was caused by a rough edge on the side of the specimen which initiated a fatigue crack. A loose wire on the feedback from the load cell controlling load on the specimen caused a third specimen to fail and the cause of the fourth specimens failure remained undetermined.

Two specimens that were different from the rest were specimen N 41 (Figure 4.6) and specimen N 43 (Figure 4.3). During testing a crack on the surface on specimen N 41 started at a point away from the hole edge. No apparent surface flaws were visible but the cause might have been due to an internal flaw which initiated a crack. Specimen N 43 was different because it was the only specimen whose initial crack did not grow to the longest crack during testing. From Figure 4.3 it can be seen that the initial crack stopped growing when its length reached 2mm and the crack on the opposite side of the hole became the longest.

From the results in Figure 4.7 it can be seen that in general the holes coldworked in this investigation required fewer number of cycles to grow cracks to 6mm than in Chandawanich's investigation. This is best explained by noting the difference in the coldworking procedure in the two investigations. In Chandawanich's experiment the fatigue cracks were initiated and grown from holes which had previously been coldworked. This is compared to the procedure of first growing the crack to a length of 1mm and then coldworking which was preformed in this report. A probable explanation of the results would then follow from the differences noted above. The hole that was mandrelized in this investigation contained a crack which may have opened and closed slightly during coldworking preventing or reducing the residual stress in the crack vicinity. This would reduce the effectiveness of the coldworking procedure as compared to mandrelizing before a crack was formed. A study of the residual strains around the coldworked hole is presented in Chapter 5 where it is shown that the residual strains are in fact smaller for the cracked hole than the residual strains for the uncracked hole in the vicinity close to the hole edge.

Ch

It

bo

Crack growth data for a noncoldworked specimen from Chandawanich is also plotted in Figure 4.7 for comparison. It is seen that coldworking can increase the fatigue life of both a cracked and a noncracked fastener hole.

CHAPTER 5

RESIDUAL STRAINS

5.1 Overview

This section presents the values of residual strains formed by coldworking a hole with an existing crack approximately 0.039 inches (1mm) long. Residual strains due to the radial expansion were measured by the moiré technique discussed in Chapter 3 and were compared to those strains obtained by Chandawanich (1) in his recent study of coldworked holes. An important point to note is that the residual strains in Chandawanich's report were measured around a coldworked hole which did not contain any cracks and in this report the hole was damaged by a crack 0.039 inches (1mm) long.

5.2 Experimental Results

Residual radial and tangential strains measured by the moiré technique are plotted in Figures 5.1 to 5.4 for both the cracked hole from this report and for the uncracked hole from Chandawanich (1). The strains in both Chandawanich's and this report were measured from a medium coldworked hole which has a range of 0.089mm to 0.102mm radial expansion.

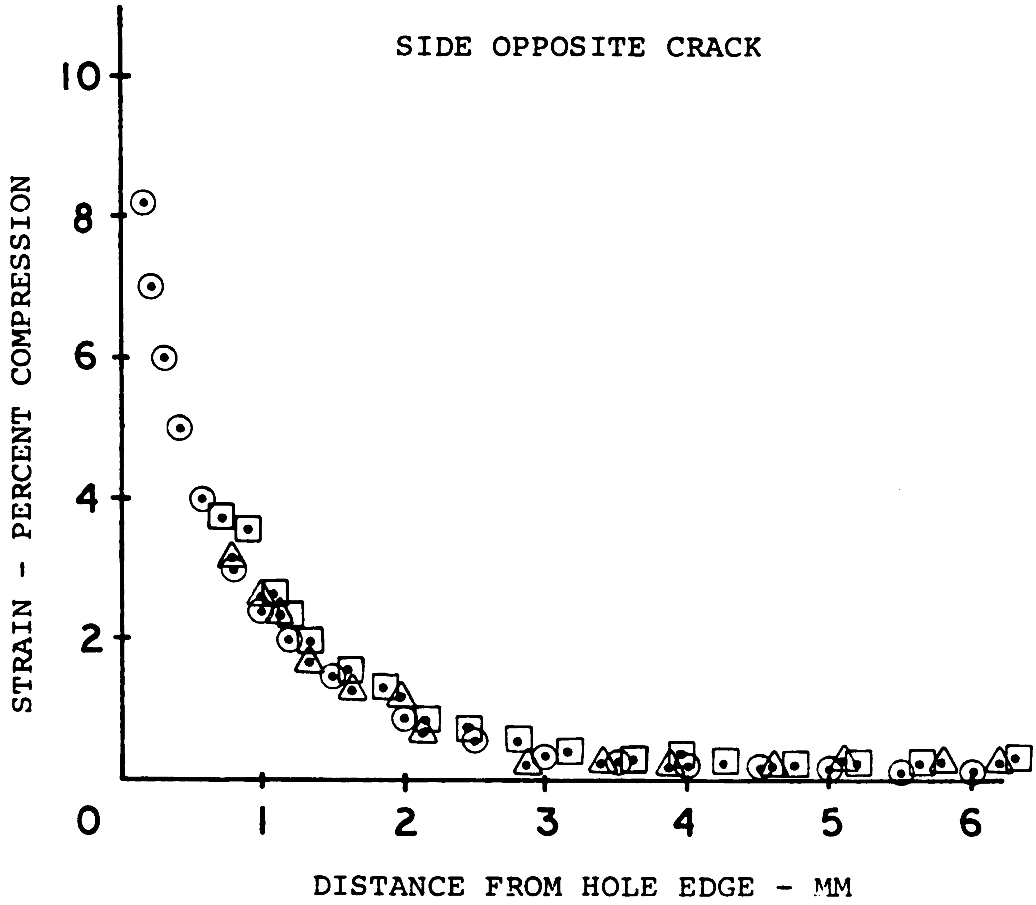

Specimen	Radial Expansion	Crack Length
⊡ N34	0.00325 inch	1.2 mm
△ N39	0.0036	0.98
⊙ Chandawanich	0.0040	No Crack

Figure 5.1 Comparison of residual radial strain with data from Chandawanich for medium coldworked hole.

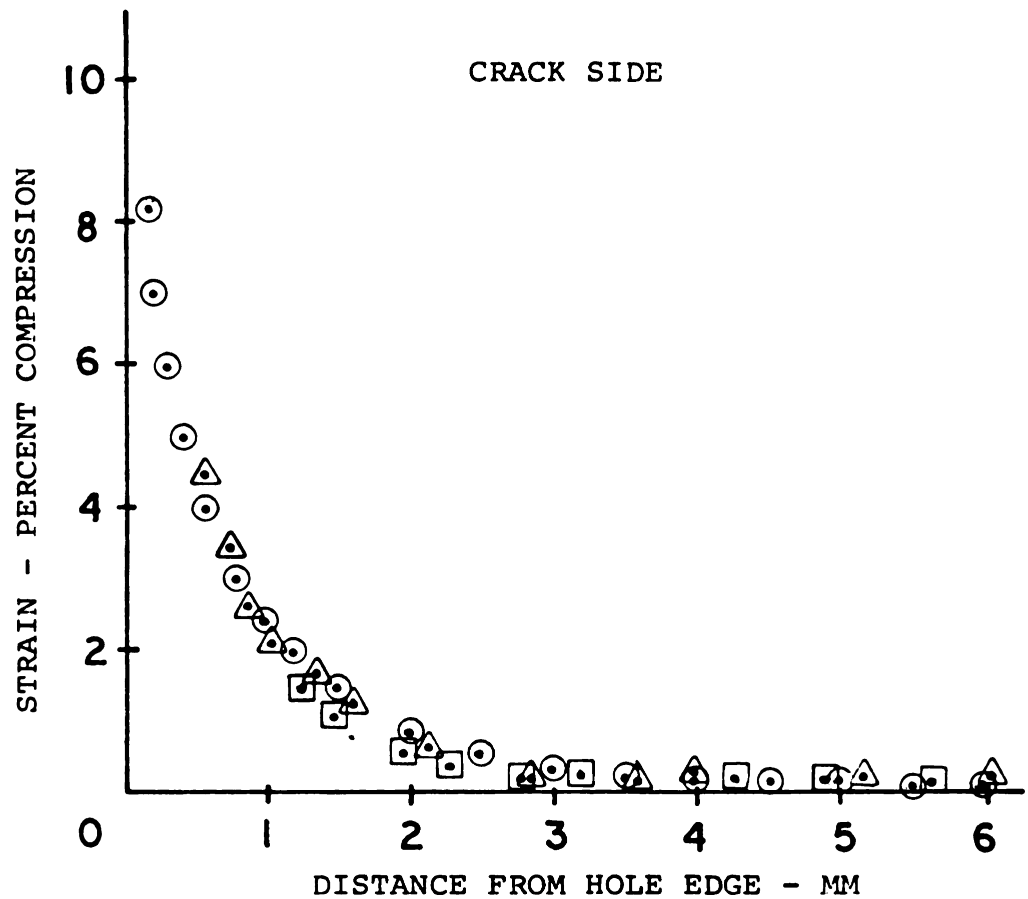

Specimen	Radial Expansion	Crack Length
⊡ N34	0.00325 inch	1.2 mm
△ N39	0.0036	0.98
⊙ Chandawanich	0.0040	No Crack

Figure 5.2 Comparison of residual radial strain with data from Chandawanich for medium coldworked hole.

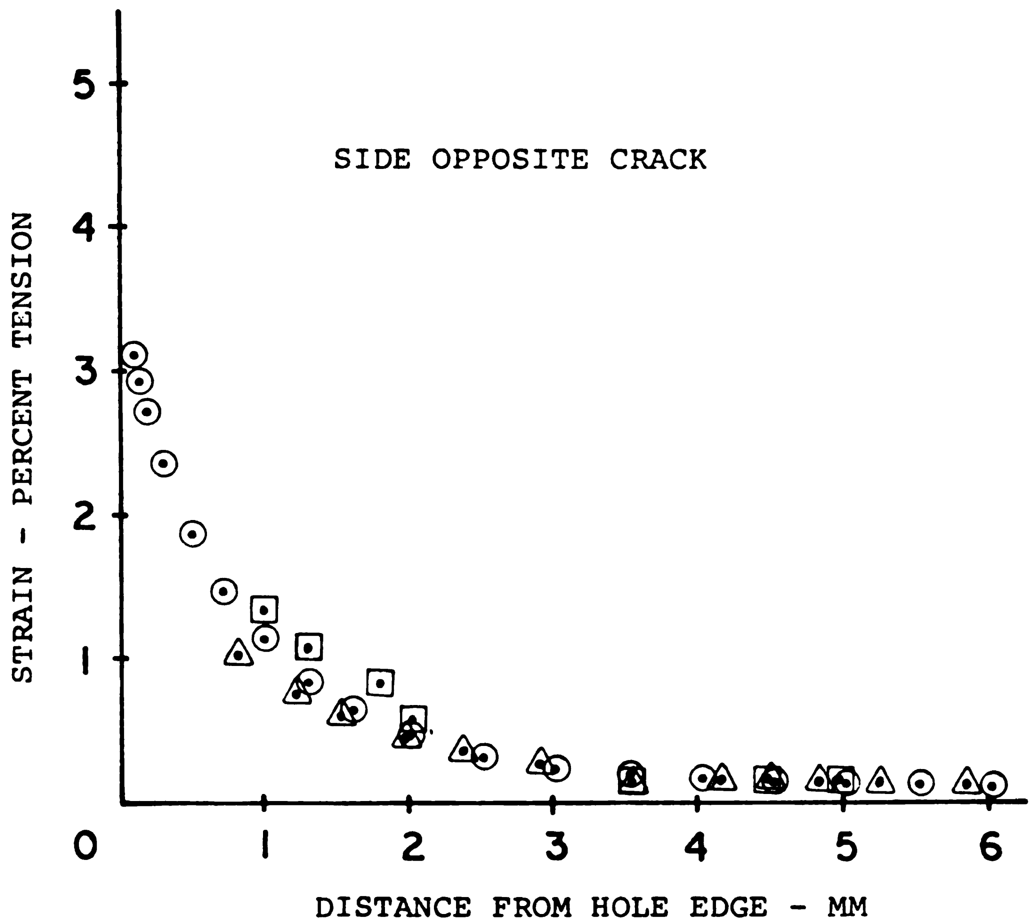

Specimen	Radial Expansion	Crack Length
⊡ N34	0.00325 inch	1.2 mm
△ N39	0.0036	0.98
⊙ Chandawanich	0.0040	No Crack

Figure 5.3 Comparison of residual tangential strain with data from Chandawanich for medium coldworked hole.

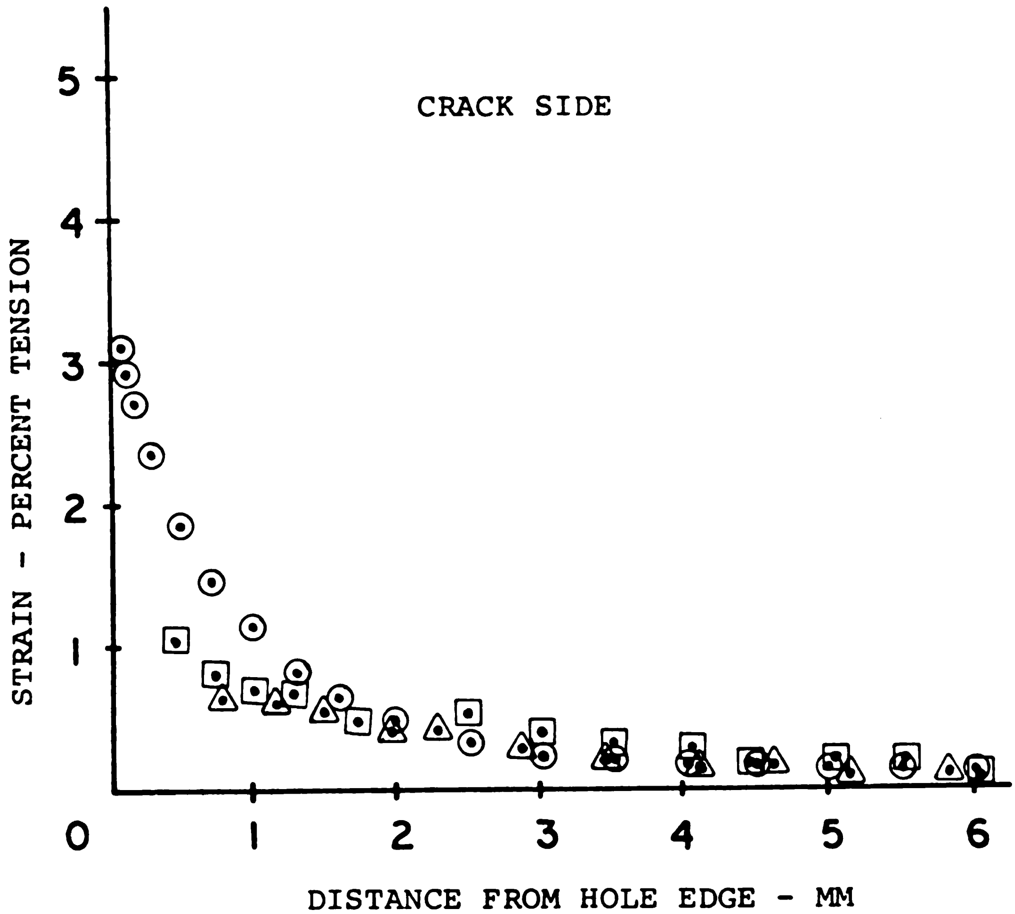

Specimen	Radial Expansion	Crack Length
⊡ N34	0.00325 inch	1.2 mm
△ N39	0.0036	0.98
⊙ Chandawanich	0.004	No Crack

Figure 5.4 Comparison of residual tangential strain with data from Chandawanich for medium coldworked hole.

The radial strains shown in Figure 5.1 were measured on the side of the hole opposite the crack and out to a distance of around 6mm. When compared to the values of Chandawanich it can be seen the agreement is very close. A radial strain of 2.55% compression was measured at 1mm dropping off to the minimum value of 1.5% compression measured at 5mm from the edge of the hole. The values of radial strain for the cracked side of the hole are shown in Figure 5.2. On this side of the hole the average radial strain values for the cracked hole can be seen to be close to the values for the uncracked hole (Chandawanich's data).

The tangential strains are shown in Figures 5.3 and 5.4. For the side opposite the crack the average value of tangential strain compares well to that of the uncracked hole. An average value of 1.2% tangential strain was measured at 1mm and 1.0% tangential strain was measured at 6mm from the hole edge. On the cracked side of the hole the tangential strains were lower when compared to the uncracked hole until at a distance of 2mm the tangential strains become equal. The strains across the crack were values measured when the crack was closed.

5.3 Discussion of Results

The results of this chapter show that the tangential residual strains were lower for the cracked specimen than the uncracked specimen (Chandawanich's data) after coldworking in the range of 0.0889mm to 0.0940mm of radial expansion. This difference is most likely due to the opening of the crack in the flawed specimen during the coldworking operation. As the mandrel was pulled through the hole the crack may have opened and closed slightly relieving the strains in the area of the crack and also ahead of the crack tip. This relief would not have been experienced by a coldworked hole without a crack and therefore higher residual strains would have formed around the perimeter of the hole.

CHAPTER 6

CRACK SURFACE DISPLACEMENT

6.1 Overview

Measurements of crack surface displacements may be used as part of a fracture criterion for classifying materials (7) as well as serving other research purposes in crack behavior. For example, experimental studies have been performed by the interferometric measurement technique for crack displacement in glass specimens. Crosley-Mostovoy-Ripling (8) and Sommer (9) used this technique for stress intensity factor calibrations. Determining the separation of fatigue crack surfaces as a function of applied load has also been investigated during recent studies of crack closure as a possible mechanism for fatigue crack retardation.

Chandawanich (1) in his recent investigation used the interferometric displacement gage described in Chapter 3 to determine crack surface displacements from cracks initiating from coldworked holes. This method developed by Sharpe-Grant (10) employs laser interferometry to measure surface displacements with a sensitivity of about 0.1 micron. It is readily adaptable to laboratory measurements and has the capability of obtaining the entire crack displacement profile. Results from Chandawanich's investigation are compared with the results of this investigation in Figures 6.2 and 6.3, which also employed the interferometric displacement gage to obtain crack surface displacements. The important difference between the two investigations is noted as follows. Chandawanich initiated and grew a crack from a coldworked hole and this report follows the growth of a crack from a hole which has been coldworked at a crack length of 1mm.

6.2 Experimental Results

The experimental data for crack displacements in this investigation were obtained from the interferometric displacement gage which produced a load-displacement curve as shown in Figure 6.1. The slope in the linear region above the crack opening load was measured, and a crack opening displacement was calculated from this slope using a 6.9MPa increment of stress. The data for the crack mouth displacements was measured from two indentations located at a distance 50 microns from the hole edge and 25 microns on either side of the crack. The results are shown in Figure 6.2. The data for the crack surface profiles was measured from two indentations located 25 microns on either side of the crack and spaced 1mm apart. These measurements were taken

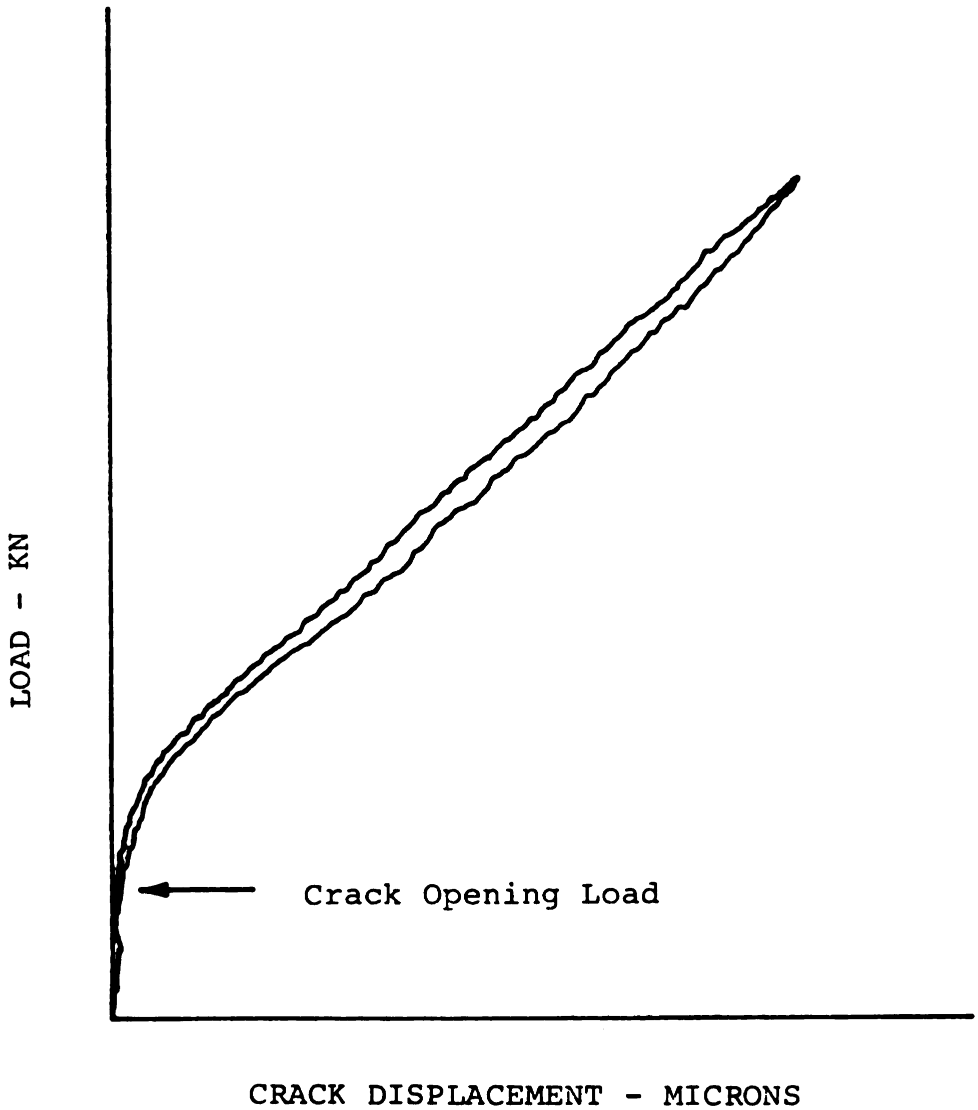

Figure 6.1 Example of load-displacement curve obtained by the Interferometric displacement gage.

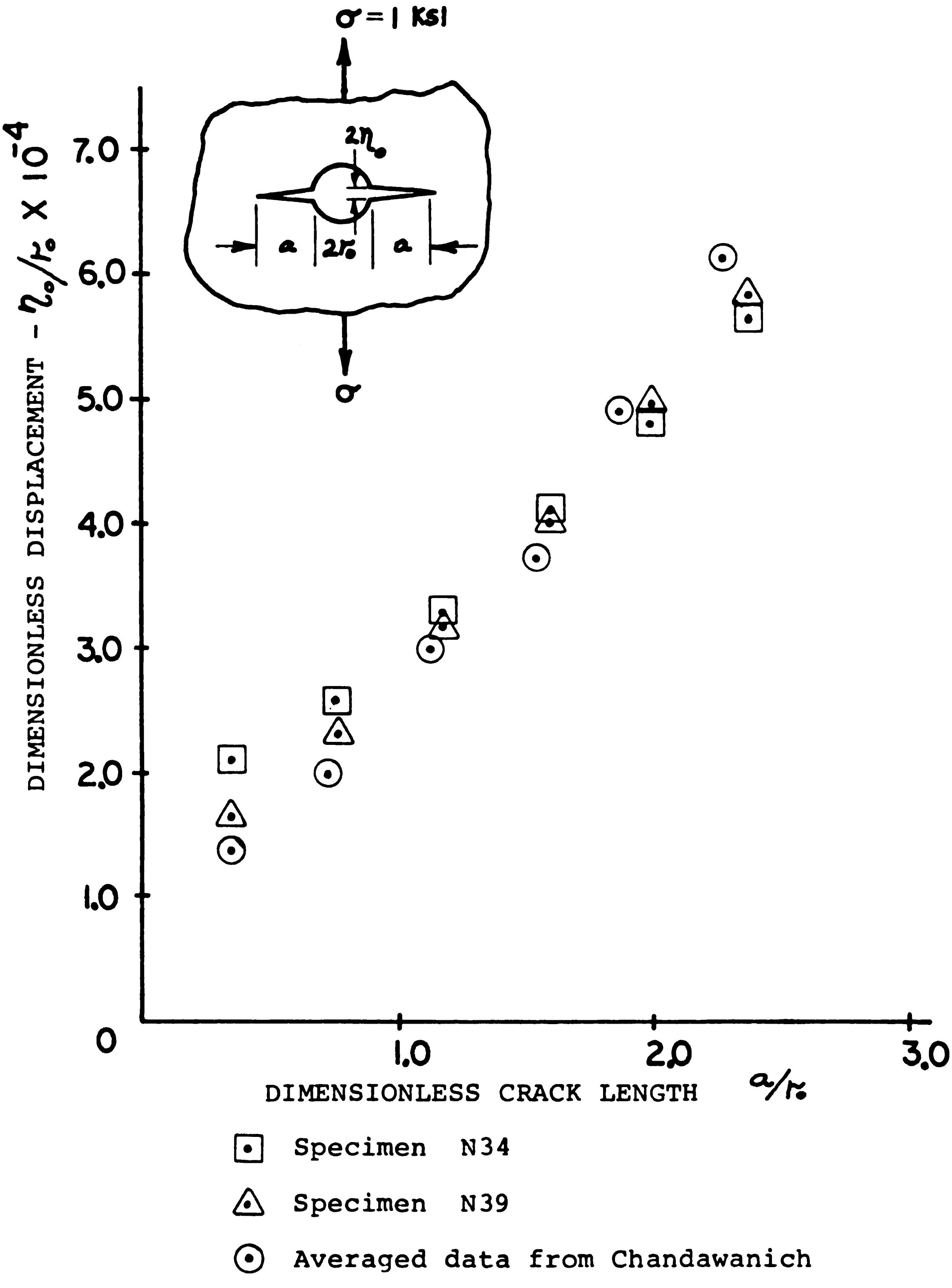

Figure 6.2 Comparison of crack mouth displacement with data from Chandawanich for medium coldworked specimens.

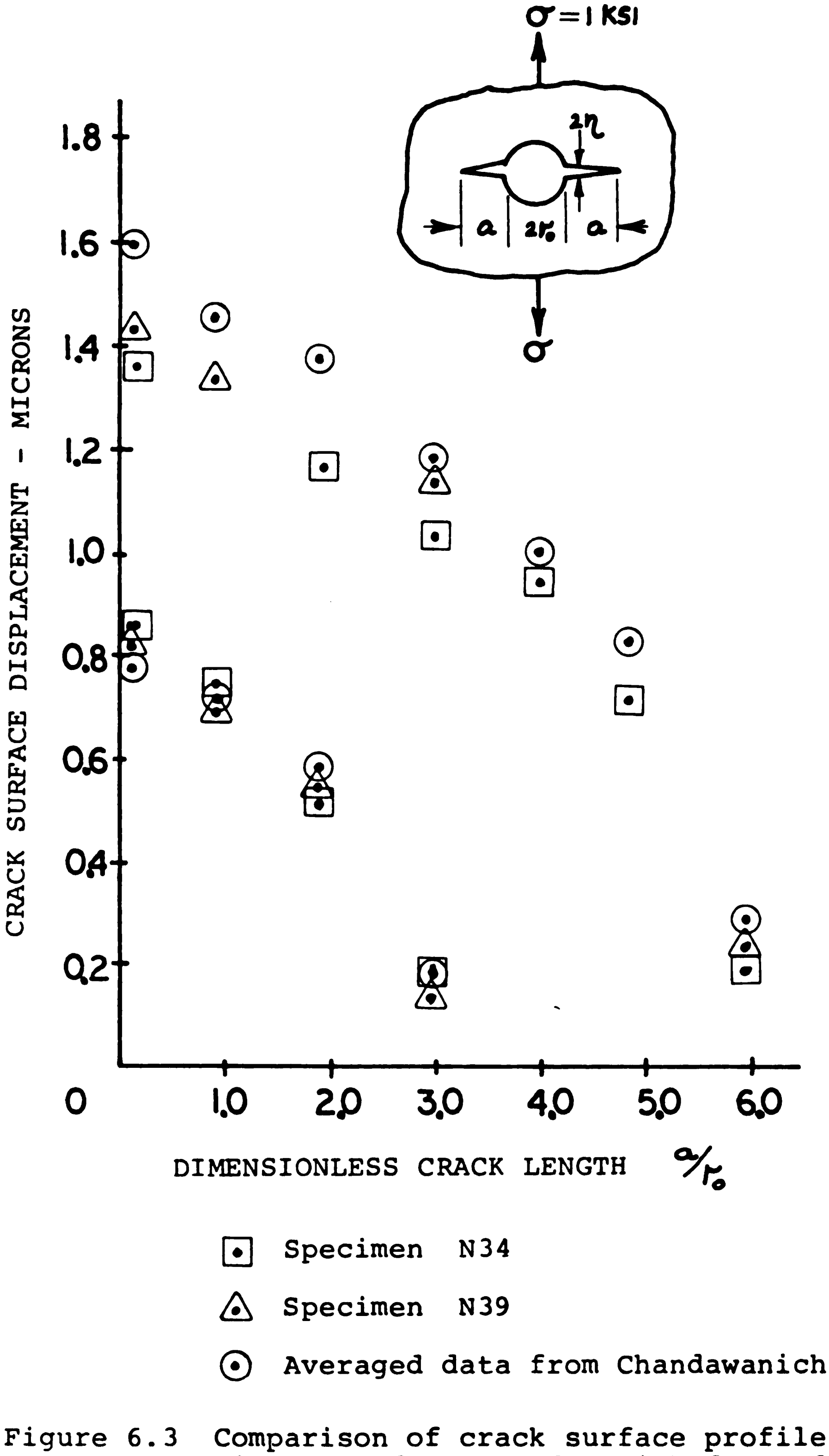

Figure 6.3 Comparison of crack surface profiles with data from Chandawanich for medium coldworked specimens.

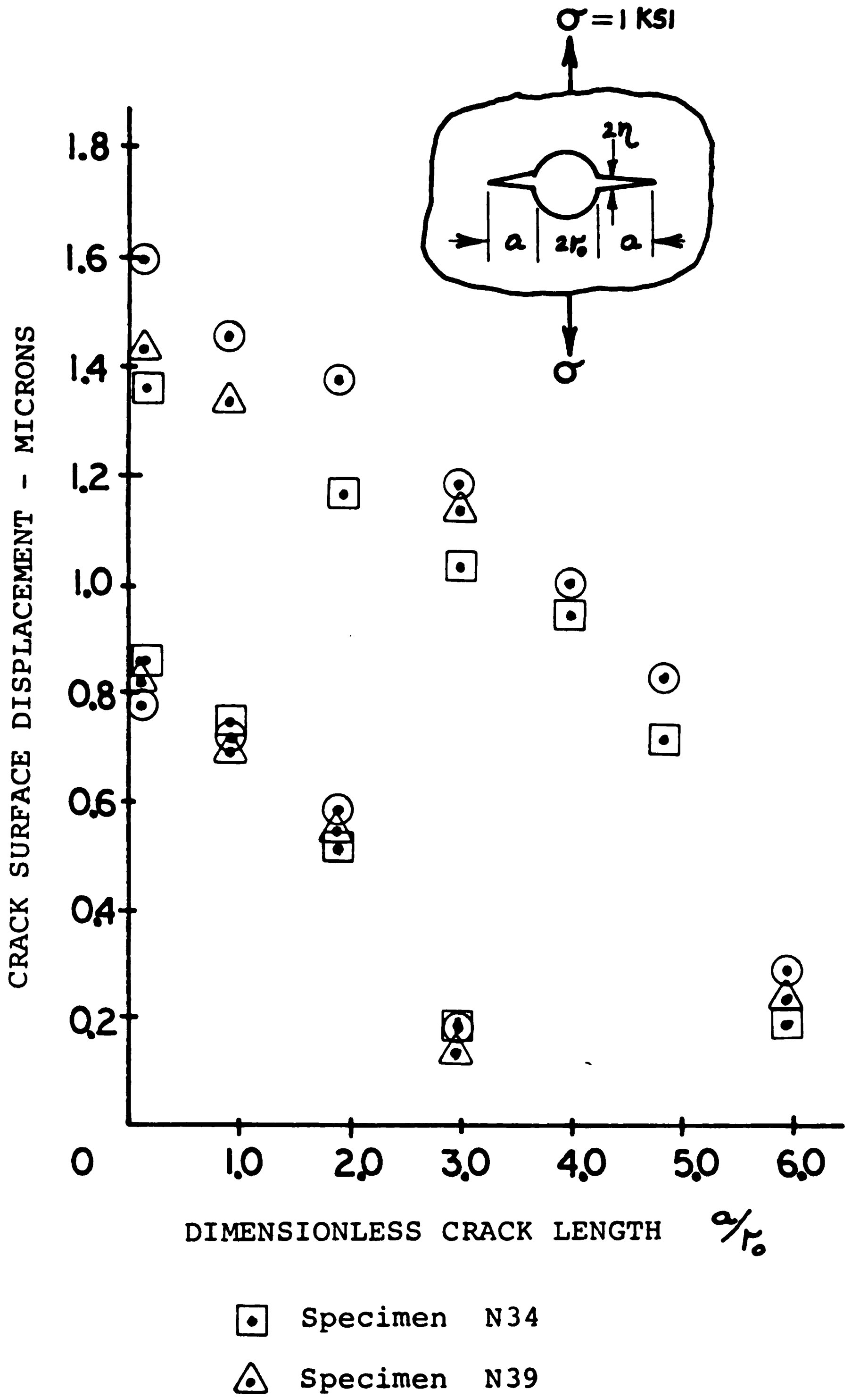

Figure 6.3 Comparison of crack surface profiles with data from Chandawanich for medium coldworked specimens.

at two different crack lengths, 3mm and 6mm and the results shown in Figure 6.3.

6.3 Discussion of Results

The two figures mentioned, 6.2 and 6.3 also contain a comparison with Chandawanich's data which is an average of the displacements from two specimens. In both graphs the data is in good agreement with each other considering the differences in the crack growth histories. Since the fatigue mechanism works on the microscopic level, duplication of crack initiation and growth is difficult to achieve. The differences in crack growth patterns may effect the crack surface displacement because a specimen which contains more cracks and cracks which are through the width of the specimen are more compliant than specimens of the opposite sense. A more compliant specimen will yield a larger crack displacement for a given load which may explain the small differences seen in Figures 6.2 and 6.3.

CHAPTER 7

STRESS INTENSITY FACTOR

7.1 Overview

In Chapter 3 the stress intensity factor, K, was shown to be inversely proportional to the slope, σ/U_y, of the load displacement curve as shown in equation 3.2.5. At a particular crack length the slope, $U_{y/\sigma}$, can be found from the IDG technique discussed in Chapter 3 and a stress intensity value calculated which then can be plotted against the crack length, a. Instead of plotting the values K and a, which depend on the dimensions and loads of the specimen, it is more useful to plot the nondimensional values,

$$\frac{K}{\sigma\sqrt{\pi a}} \text{ and } \frac{a}{r_o},$$

where K Stress intensity factor.

σ = Remote load.

a = Crack length.

r_o = Radius of hole in specimen.

Using the nondimensionalized values allows the results to be duplicated without the necessity of duplicating the specimen size and loads.

The results in this chapter are compared to the experimental results of Chandawanich (1) who preformed a similar study of stress intensity versus crack length but used a different procedure in preparing the specimen. The mandrelizing was preformed on a hole with no cracks, as compared to mandrelizing a hole with a 1mm crack as was done in this experiment.

7.2 Experimental Results

Data in this experiment was taken from indentations placed at 25 microns on either side of a fatigue crack grown from a coldworked hole. The indentations were 50 microns from the tip of the crack and placed at crack growth intervals of 1mm. The crack length after coldworking was approximately 1mm and was grown to a final length of 6mm in 1mm increments.

The final nondimensionalized values for the stress intensity factors are shown in Figure 7.1 as a function of the nondimensional crack length. Averaged values from Chandawanich (1) has also been plotted. It can be seen that the data for the cracked hole agrees well with Chandawanich's data for a noncoldworked hole, which indicates the coldworking of the cracked hole had little effect on the stress intensity values.

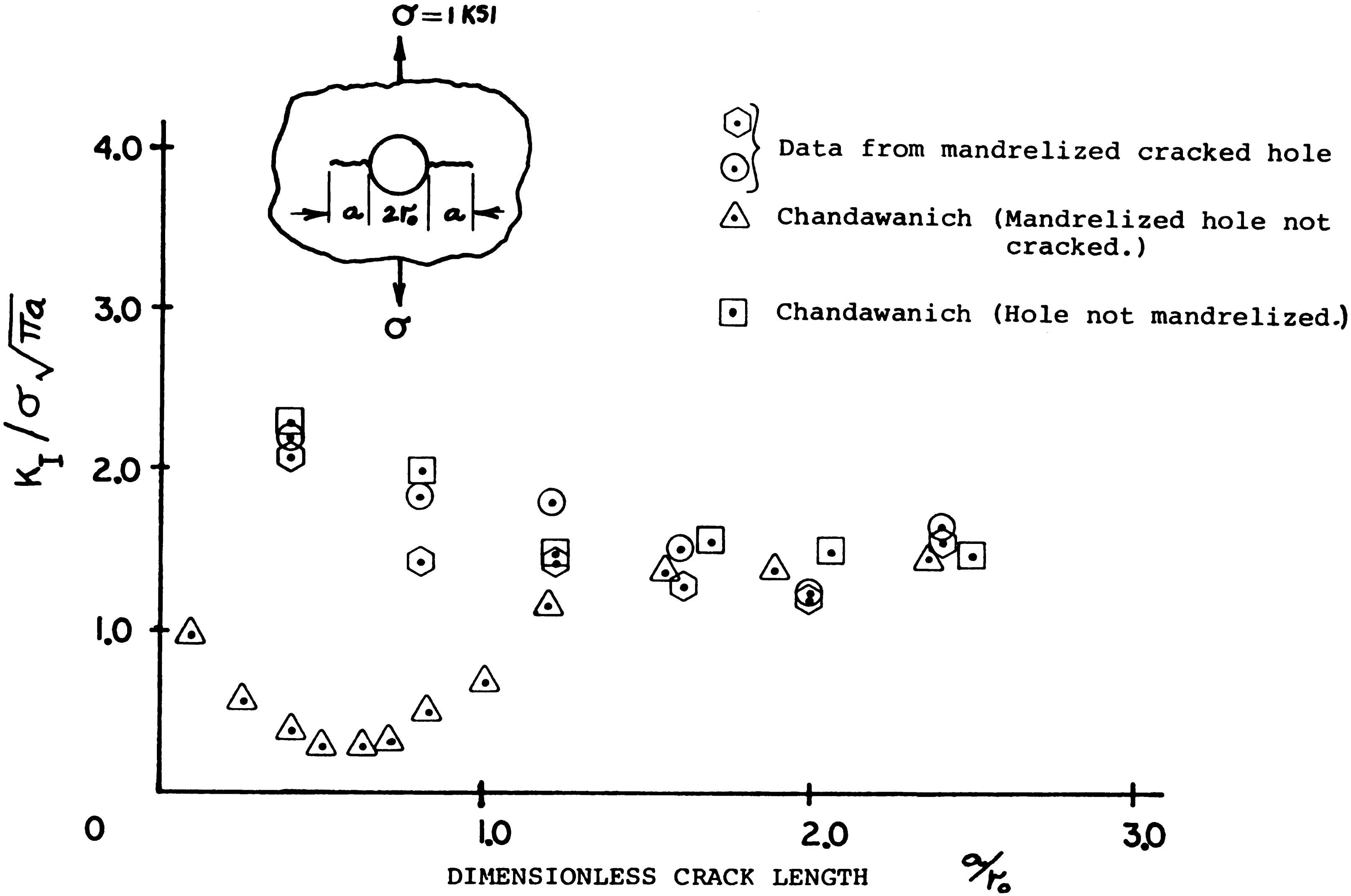

Figure 7.1 Comparison of stress intensity factor with data from Chandawanich.

7.3 Discussion of Results

Three different types of holes have been compared in Figure 7.1, a hole which was precracked to a length of 1mm and coldworked, a hole which was coldworked but not precracked, and a hole which was neither coldworked or precracked. The latter two were obtained by Chandawanich (1). The results show in Figure 7.1 that the relationship for the cracked coldworked hole does not differ much from a hole which has not been coldworked or cracked and the results for all three types of holes agree well after a ratio of a/r of about 1.3.

It was shown in previous chapters that the residual strains for the coldworked holes dropped off rapidly to a hole edge distance of 3mm and then level off to a value of 0.02% strain, see Figures 5.1 to 5.4. This distance from the hole edge of 3mm corresponds very closely to a crack length of 0.126 inches (3.2mm) found from the ratio a/r_o when it equals 1.3, which is the value where the stress intensity factor is the same for the three different types of holes described in this chapter. This shows that when the residual strains become very small at a distance of about 3mm from the hole edge the stress intensity factor compares well to that of a hole which has not been coldworked.

CHAPTER 8

CONCLUSIONS

It was found from this investigation that specimens containing holes of a specified size, and coldworked with the same process, are nearly identical with the exception of the crack growth curves. The specimen holes were mandrelized to produce a medium amount of coldworking, 0.089mm to 0.104mm radial expansion, after a 1mm crack had been grown. Cracks were grown to 6mm lengths from the hole edge by fatigue. Fatigue tests were restricted to 3.2mm thick specimens, a hole size of 4.98mm, and constant-amplitude cyclic loading of 33375N maximum and 3337.5N minimum.

The specimens when coldworked and tested in the above manner produced crack growth curves which varied from each other by as much as 2.5×10^5 cycles. Crack growth data from Chandawanich (1) when compared to data in this report showed that the number of cycles to produce a 6mm crack in a coldworked hole without an initial crack was 3½ times the number of cycles of a coldworked hole with a 1mm crack. In all specimens tested it was shown that the number of cycles to grow a crack to 6mm exceeded that of a noncoldworked hole. This has shown that the coldworking technique can be useful in extending the life of a part subjected to fatigue.

Sleeves which were left in two of the specimens after coldworking were also tested. One of these specimens fractured at a crack length of 1.1mm. Since this crack had only grown 0.1mm during the test, a complete crack growth curve to a 6mm crack length could not be plotted. The second specimen tested did not fracture and resulted in a crack growth curve similar to specimens in which the sleeve was removed. It was concluded that the presence of the sleeve after coldworking a hole which contained a 1mm crack does not affect the crack growth.

The moiré technique was a very useful method in measuring the residual strains around the coldworked holes. The results were reproducible and the technique as applied in this investigation could measure strains as close as 0.5mm from the hole edge. The results of the moiré technique were presented in Chapter 5. From the comparison made to Chandawanich's data in this chapter it was shown that the residual strains around a coldworked hole containing a 1mm crack are nearly the same for a coldworked hole not containing a crack. It can be concluded from this chapter that repairing a hole with a small crack by mandrelizing the hole can produce nearly the same residual strains as mandrelizing a hole without a crack.

The experimental results of the crack surface displacements were obtained by the IDG technique and agreed well with with the data from Chandawanich. This agreement has shown that the surface displacements of a fatigue crack that was present when the hole was coldworked are the same as the surface displacements of a fatigue crack not existing when the hole was coldworked. It is therefore concluded that the presence of the crack during the coldworking operation does not affect the crack surface displacements measured after crack growth.

The stress intensity factor was also found by the use of the IDG technique for a fatigue crack which existed when the hole was coldworked. The results agreed very closely to the data of a noncoldworked hole obtained by Chandawanich, and were larger than the values for a hole which did not contain a crack when coldworked. Therefore the presence of the crack during the coldworking operation made it comparable to the noncoldworked hole.

It can be concluded that the mandrelization process can be used to extend the fatigue life of a fastener hole containing a small fatigue crack (1mm). This fatigue life is, in general, much less than the fatigue life of a coldworked hole without an initial crack, but is greater than the fatigue life of a noncoldworked specimen. Mandrelization can, therefore, be used as a repair operation on cracked fastener holes.

REFERENCES

1) Chandawanich, N. "An Experimental Study of Crack Initiation and Growth From Coldworked Holes," a Doctoral Dissertation, Michigan State University, Department of Metallurgy, Mechanics and Materials Science, 1977.

2) Speakman, E. R. "Fatigue Life Improvement Through Stress Coning Methods," American Society for Testing and Materials, STP 467, September 1970, pp. 209-227.

3) Gerber, T. L. and H. O. Fuchs. "Improvement in the Fatigue Strength of Notched Bars by Compressive Self-Stresses," STP 467, September 1970, pp. 276-294.

4) Sharpe, W. N., Jr. "Measurements of Residual Strains Around Coldworked Fastener Holes," AFOSR-TR-77-0020, April 1976.

5) Sharpe, W. N., Jr. "Interferometric Surface Strain Measurement," International Journal of NonDestructive Testing, Vol. 3, 1971, pp. 56-76.

6) Sharpe, W. N. and D. R. Martin. "Optical Measurements of In-plane Strain/Displacement Near Crack Tips at High Temperature," a paper presented and published at the 6th International Conference on Experimental Stress Analysis, Munich, Sept. 18-22, 1978.

7) Rolge, S. T. and J. M. Barsom. Fracture and Fatigue Control in Structures, Applications of Fracture Mechanics. Prentice-Hall, Inc., Englewood Cliffs, New Jersey, 1977, pp. 27.

8) Crosley, P. B., S. Mostovoy, and F. J. Ripling. "An Optical-Interference Method for Experimental Stress Analysis of Cracked Structures," Engineering Fracture Mechanics, Vol. 4, No. 3, 1971, pp. 421-433.

9) Sommer, E. "An Optical Method for Determining the Crack-Tip Stress Intensity Factor," Engineering Fracture Mechanics, Vol. 1, 1970, pp. 705-718.

10) Sharpe, W. N., Jr. and A. F. Grant, Jr. "A Preliminary Study of Fatigue Crack Retardation Using Laser Interferometry to Measure Crack Surface Displacements," Technical Report AFML-TR-74-203, Wright-Patterson Air Force Base, Ohio 45433, March 1975.